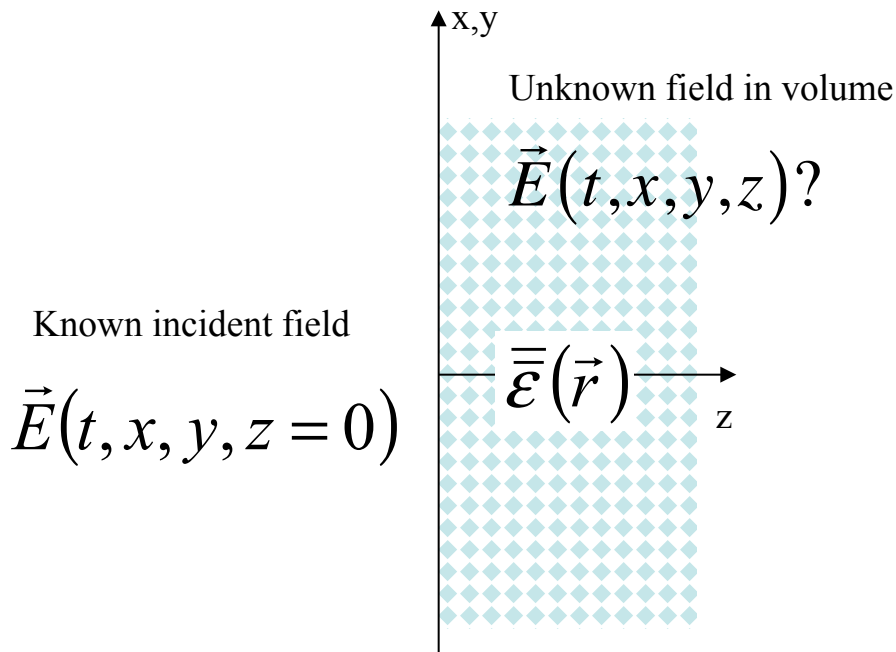


Beam Propagation

Statement of problem

Now let the inhomogeneity be strong such that the Born approximation is not valid. We will now use an iterative solution that propagates through the space in small steps Δz



As long as each small slice obeys certain conditions (one of which is again the Born approximation) we can accommodate strong scattering in the volume. The penalty is that the solution is not perfectly accurate for non-paraxial rays. There are modifications that solve this limit.

Beam propagation

Derivation of scalar solution (1/3)

Approximations in **red**, numerical constraints in **blue**.

From the method of undetermined coefficients and the **SVEA**, we have

$$E(t, x, y, z) = \mathcal{F}_{txy}^{-1} \left\{ \mathcal{E}(\omega, k_x, k_y, z) e^{-jk_z(\omega, k_x, k_y)z} \right\}$$

$$2jk_z \frac{d}{dz} \mathcal{E} = k_0^2 \left[\mathcal{E}_{IH}(\omega, K_x, K_y, z) *_{k_x, k_y} E(\omega, k_x, k_y, z) \right] e^{+jk_z z}$$

Substitute the Fourier transform of the first into the second

$$2jk_z \frac{d}{dz} \mathcal{E} = k_0^2 \left[\mathcal{E}_{IH}(\omega, K_x, K_y, z) *_{k_x, k_y} \left\{ \mathcal{E}(\omega, k_x, k_y, z) e^{-jk_z(\omega, k_x, k_y)z} \right\} \right] e^{+jk_z z}$$

Let the step size z be sufficiently small that $\exp(-jk_z z)$ can be treated as invariant with k_x and k_y . Physically, this means the incident (inside brackets) and diffracted (outside) envelopes all propagate with the same phase and thus *no diffraction occurs*.

$$\frac{d}{dz} \mathcal{E}(\omega, K_x, K_y, z) = \frac{k_0^2}{2jk_z} \left[\mathcal{E}_{IH}(\omega, K_x, K_y, z) *_{k_x, k_y} \left\{ \mathcal{E}(\omega, k_x, k_y, z) e^{-jn_H k_0 z} \right\} \right] e^{+jn_H k_0 z}$$

$$= \frac{k_0^2}{2jk_z} \left[\mathcal{E}_{IH}(\omega, K_x, K_y, z) *_{k_x, k_y} \mathcal{E}(\omega, k_x, k_y, z) \right]$$

Assume $k_z(\omega, k_x, k_y) \approx n_H k_0$ for the k_z term in the denominator. Physically, $n_H k_0 / k_z = 1/\cos\theta$ which is a projection factor that accounts for extra path length of angled rays, **thus non-paraxial rays interact with the material as if they were normal incidence**. Finally, inverse transform in the transverse coordinates:

$$\frac{d}{dz} E(t, \vec{r}) = -j \frac{k_0}{2n_H} \mathcal{E}_{IH}(t, \vec{r}) E(t, \vec{r})$$

Beam propagation

Derivation of scalar solution (2/3)

Change from dielectric to index perturbation:

$$\begin{aligned}\varepsilon_H + \varepsilon_{IH}(t, \vec{r}) &= [n_H + n_{IH}(t, \vec{r})]^2 = n_H^2 + 2n_H n_{IH}(t, \vec{r}) + \cancel{n_{IH}^2(t, \vec{r})} \\ \therefore \varepsilon_{IH}(t, \vec{r}) &\approx 2n_H n_{IH}(t, \vec{r})\end{aligned}$$

to get a DE for the fields

$$\frac{d}{dz} E(t, \vec{r}) = -jk_0 n_{IH}(t, \vec{r}) E(t, \vec{r})$$

whose solution is

$$\begin{aligned}E(t, x, y, z + \Delta z) &= E(t, x, y, z) \exp \left[-jk_0 \int_z^{z+\Delta z} n_{IH}(t, \vec{r}) dz \right] \\ &\approx E(t, x, y, z) \exp \left[-jk_0 n_{IH} \left(t, x, y, z + \frac{\Delta z}{2} \right) \Delta z \right]\end{aligned}$$

Physically, this treats the inhomogeneous index as a thin transmission function via projection in a small step Δz . If the perturbation is zero, we obtain the solution that the field is invariant in z , as expected from the approximations made.

This is equivalent to the homogeneous solution in which envelopes do not change with z and that we have left diffraction out of the solution above by assuming that there is no diffraction via $\exp(-j k z z) = \text{constant}$. The evolution of the envelopes can be found by Fourier transforming the solution above:

$$\mathcal{E}(\omega, k_x, k_y, z + \Delta z) = \mathcal{F}_{txy} \left[E(t, x, y, z) e^{-jk_0 n_{IH} \left(t, x, y, z + \frac{\Delta z}{2} \right) \Delta z} \right]$$

Beam propagation

Derivation of scalar solution (3/3)

Diffraction results when we insert the solution for the evolution of the envelopes back into the solution assumed in the method of undetermined coefficients:

$$E(t, x, y, z) = \mathcal{F}_{txy}^{-1} \left\{ \mathcal{E}(\omega, k_x, k_y, z) e^{-jk_z(\omega, k_x, k_y)z} \right\}$$

To apply this formula, **we must now assume that the envelopes don't change significantly over Δz** . That is, the refraction must not change the fields significantly while we are doing the diffraction step.

Plugging the previous solution into the above, we get an iterative solution that advances the fields by one Δz

$$\begin{aligned} E(t, x, y, z + \Delta z) &= \mathcal{F}_{txy}^{-1} \left\{ E(\omega, k_x, k_y, z + \Delta z) e^{-jk_z(\omega, k_x, k_y)\Delta z} \right\} \\ &= \mathcal{F}_{txy}^{-1} \left\{ \mathcal{F}_{txy} \left[E(t, x, y, z) e^{-jk_0 n_{IH} \left(t, x, y, z + \frac{\Delta z}{2} \right) \Delta z} \right] e^{-jk_z(\omega, k_x, k_y)\Delta z} \right\} \end{aligned}$$

which is the final result.

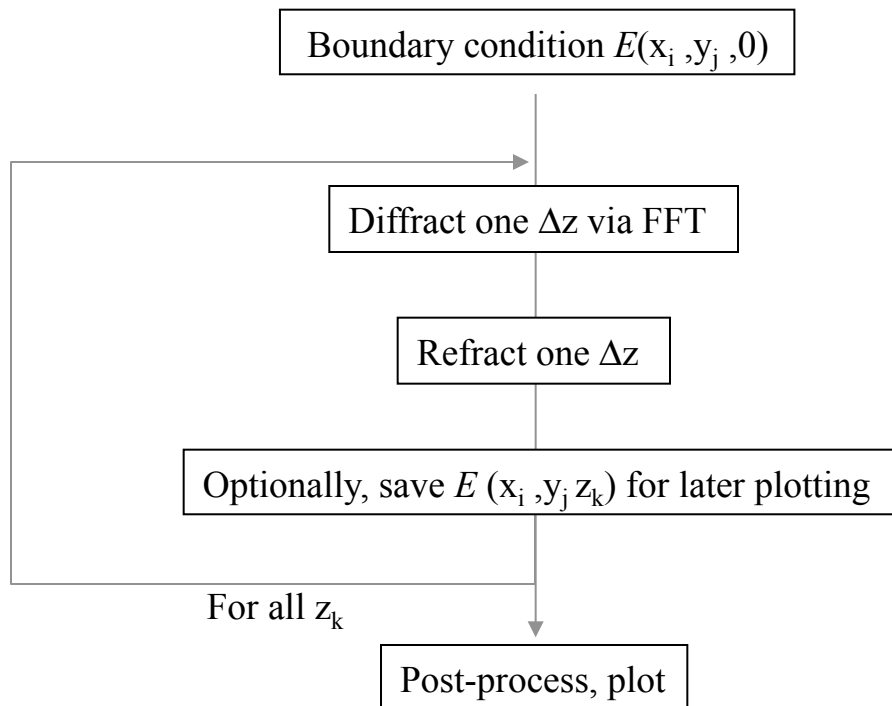
Beam propagation

Basic algorithm

This iterative solution switches back and forth between real space where refraction is applied and Fourier space where diffraction is calculated. It is thus often referred to as the Fourier split-step method

$$E(t, x, y, z + \Delta z) = \mathcal{F}_{txy}^{-1} \left\{ \mathcal{F}_{txy} \left[E(t, x, y, z) e^{-jk_0 n_{IH} \left(t, x, y, z + \frac{\Delta z}{2} \right) \Delta z} \right] e^{-jk_z(\omega, k_x, k_y) \Delta z} \right\}$$

Refraction
Diffraction



Grin lens

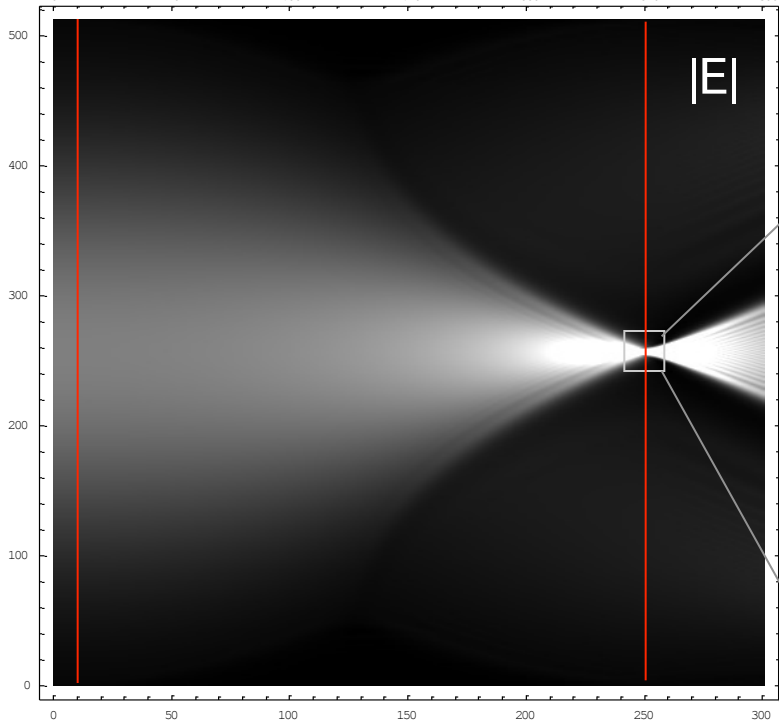
Half pitch 1 x 2.4 mm



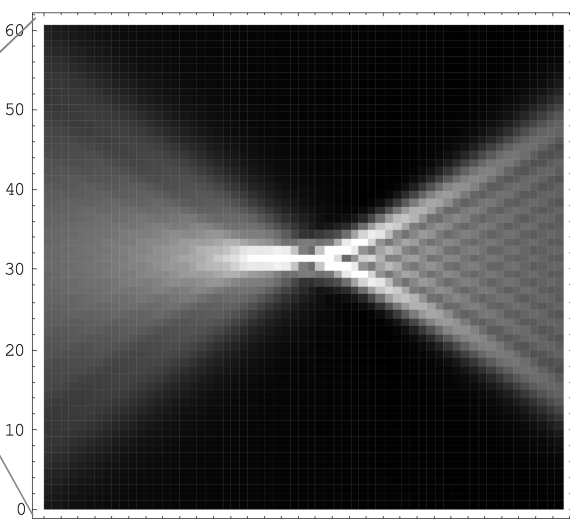
Transverse sampling
512 steps of $2 \lambda_0 = 2 \mu\text{m}$

Longitudinal sampling
300 steps of $10 \mu\text{m}$

$$\delta n(x, z) = 0.07 \cos\left(\frac{2\pi}{L_x} x\right) \operatorname{rect}\left(\frac{z - 1300}{2400}\right)$$

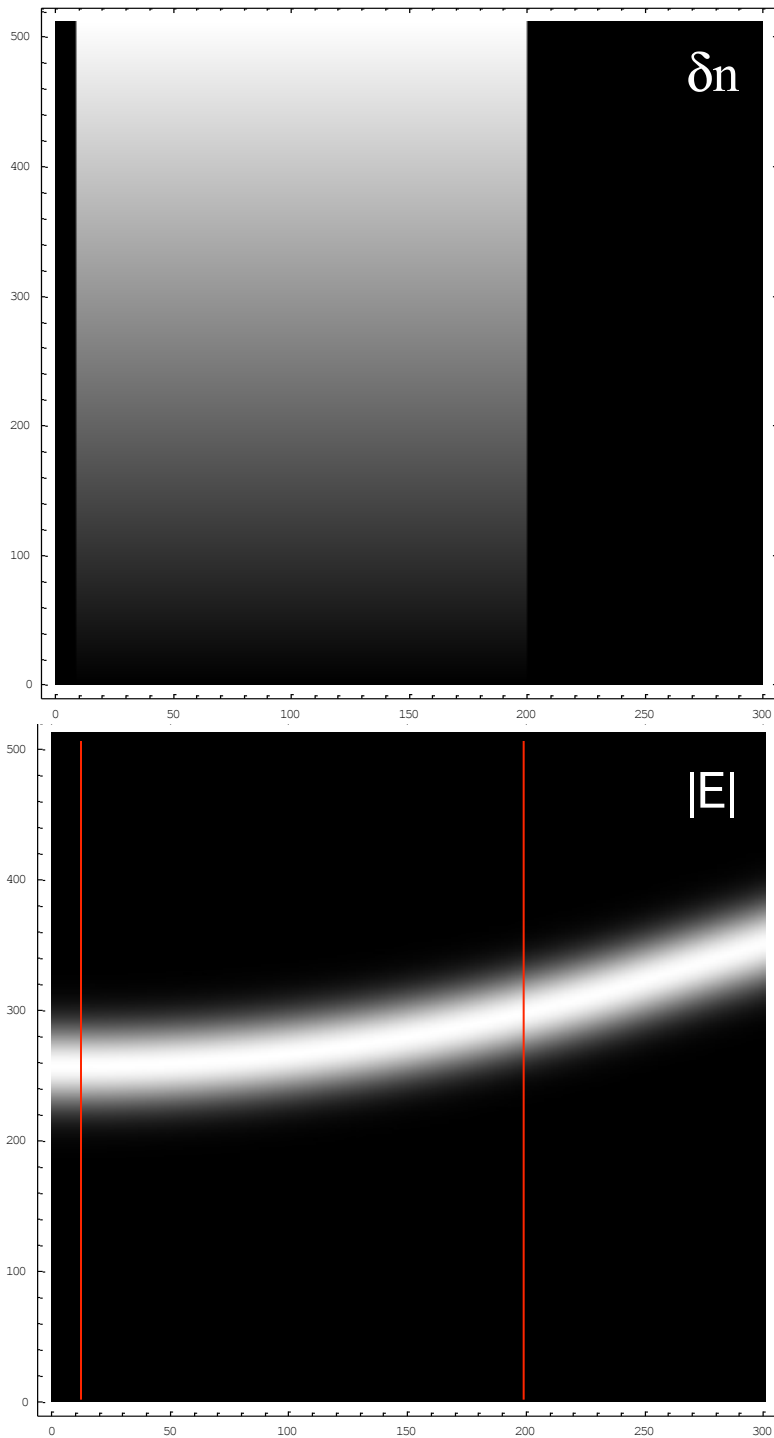


$$E(x, 0) = e^{-\left(\frac{x}{300}\right)^2}$$



Linear (Gradium) glass

Simple way to implement prisms



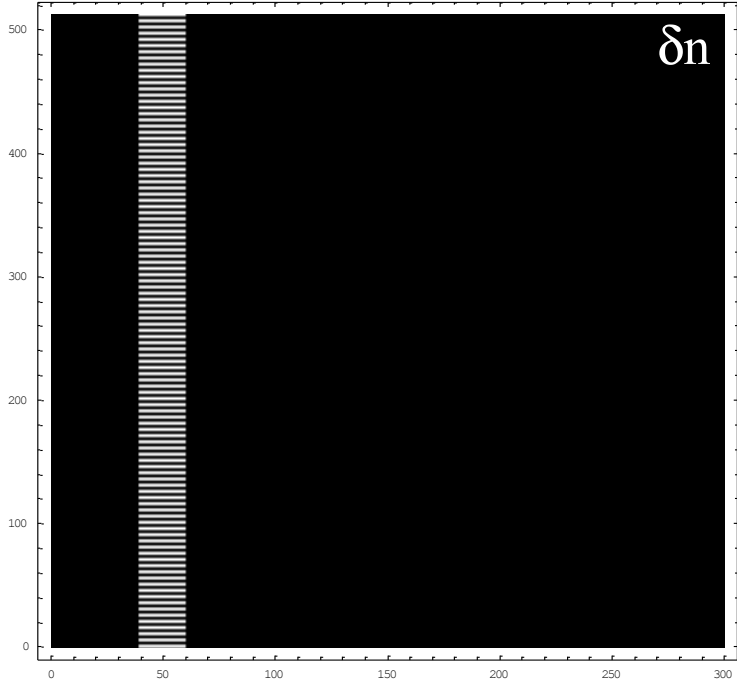
Transverse sampling
512 steps of $2 \lambda_0 = 2 \mu\text{m}$

Longitudinal sampling
300 steps of $10 \mu\text{m}$

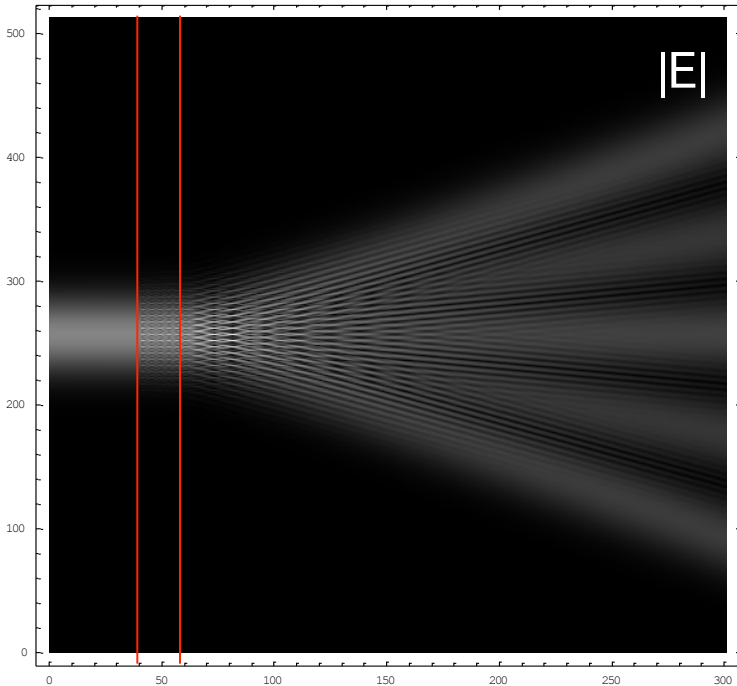
$$\delta n(x, z) = 0.07 \left(\frac{x}{L_x} \right) \text{rect} \left(\frac{z - 1050}{1900} \right)$$

$$E(x, 0) = e^{-\left(\frac{x}{60}\right)^2}$$

Thin phase grating



Transverse sampling
512 steps of $2 \lambda_0 = 2 \mu\text{m}$

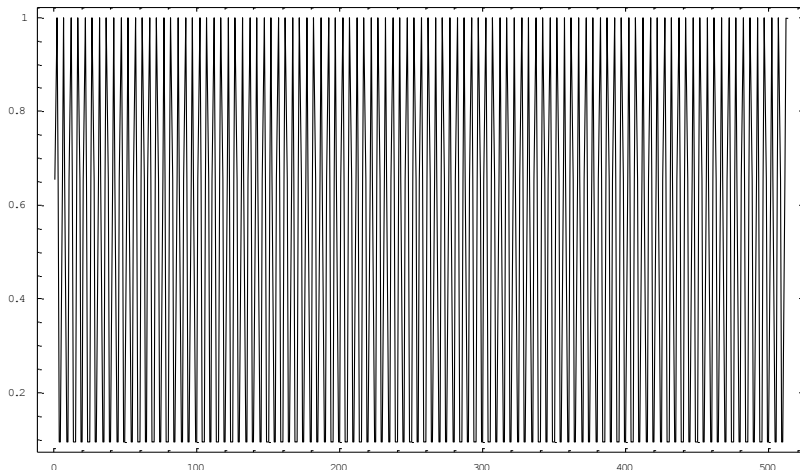


$$\delta n(x, z) = 0.07 \operatorname{rect}\left(\frac{z-500}{200}\right) \frac{\cos\left(\frac{2\pi}{10}x\right) + 1}{2}$$

$$E(x, 0) = e^{-\left(\frac{x}{60}\right)^2}$$

Thin amplitude grating

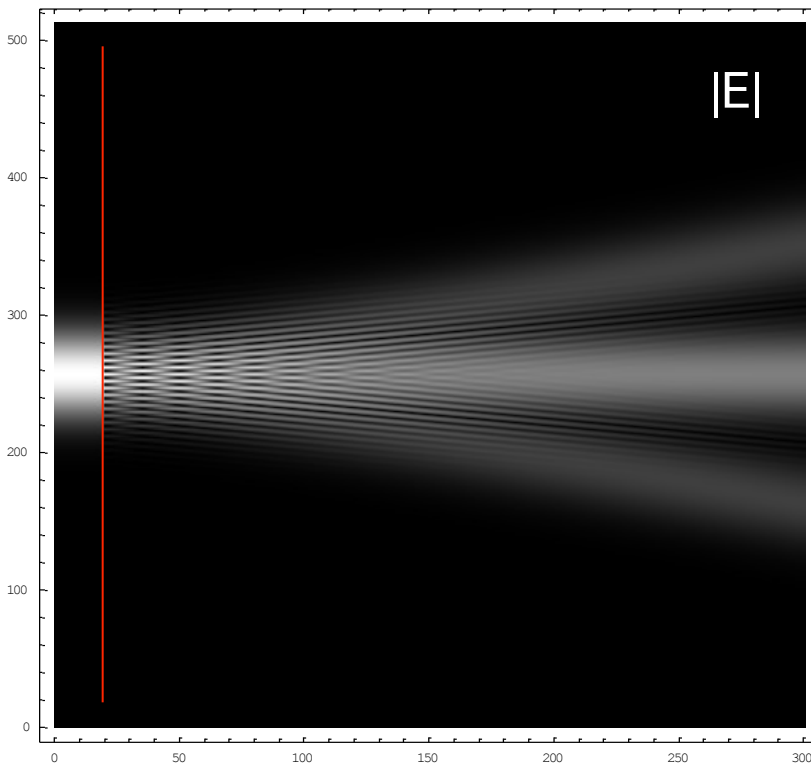
Amplitude mask at z=200



Transverse sampling
512 steps of $2 \lambda_0 = 2 \mu\text{m}$

Longitudinal sampling
300 steps of 10 μm

$$A(x,z) = \frac{\cos\left(\frac{2\pi}{10}x\right) + 1}{2}$$

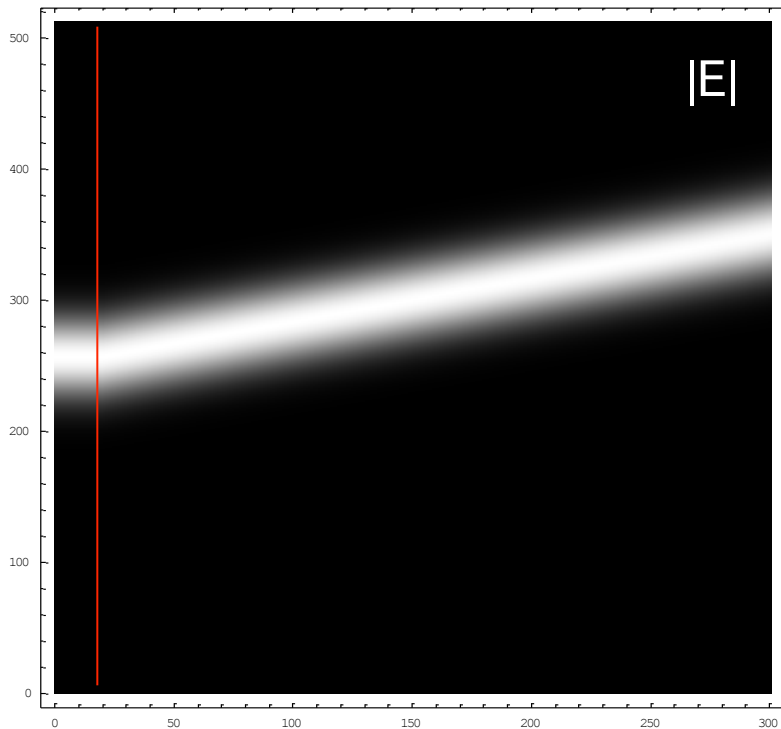


$$E(x,0) = e^{-\left(\frac{x}{60}\right)^2}$$

Zero order since DC component to mask

Gratings implemented in Fourier-space

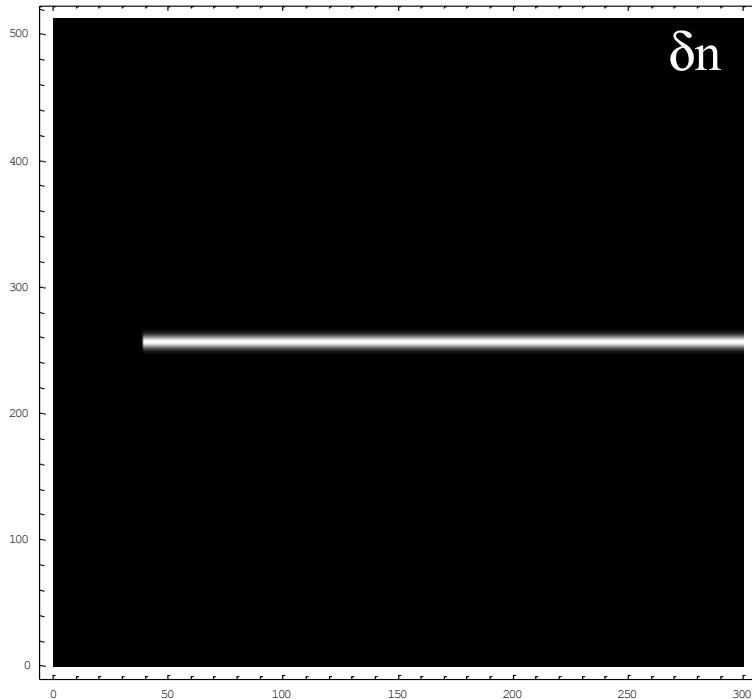
At $z=200 \mu\text{m}$ shift Fourier spectrum by $\frac{2\pi}{10} / \delta k_x$
to implement a single side-band grating



$$E(x,0) = e^{-\left(\frac{x}{60}\right)^2}$$

Jaram and Banerjee use this to simulate an AO device on page 253
of their textbook.

Waveguide

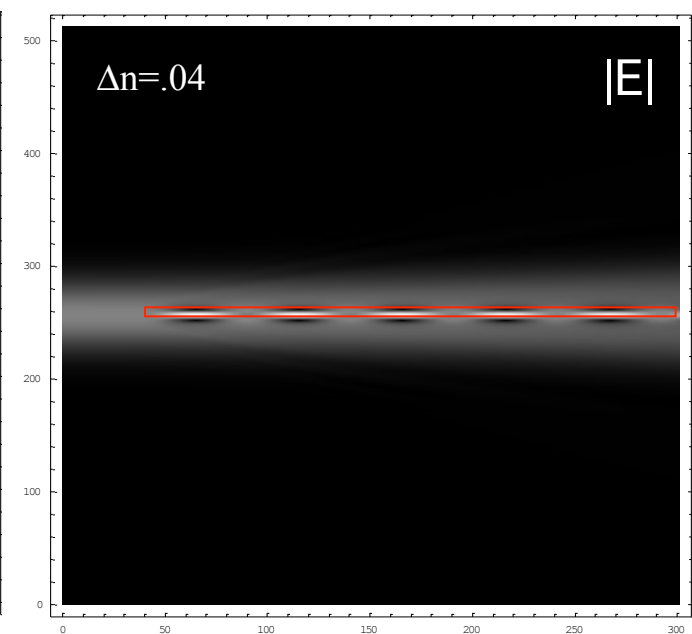
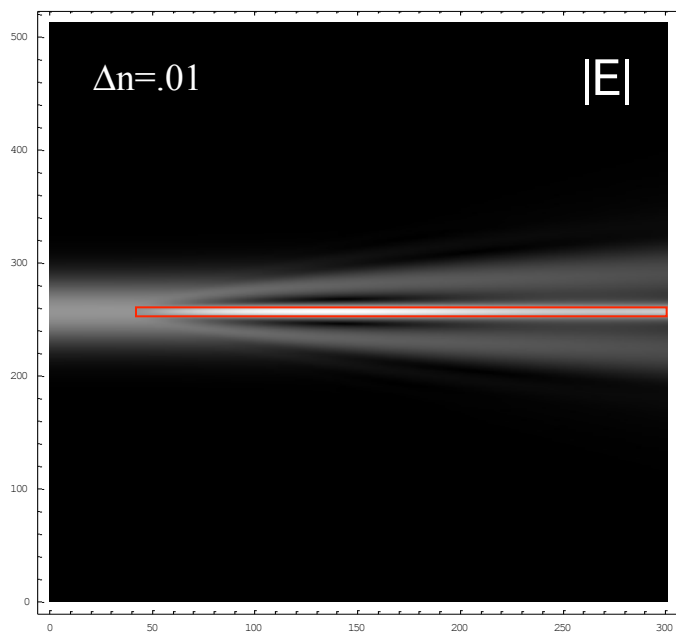


Transverse sampling
512 steps of $\lambda_0 = 1 \mu\text{m}$

Longitudinal sampling
300 steps of $10 \mu\text{m}$

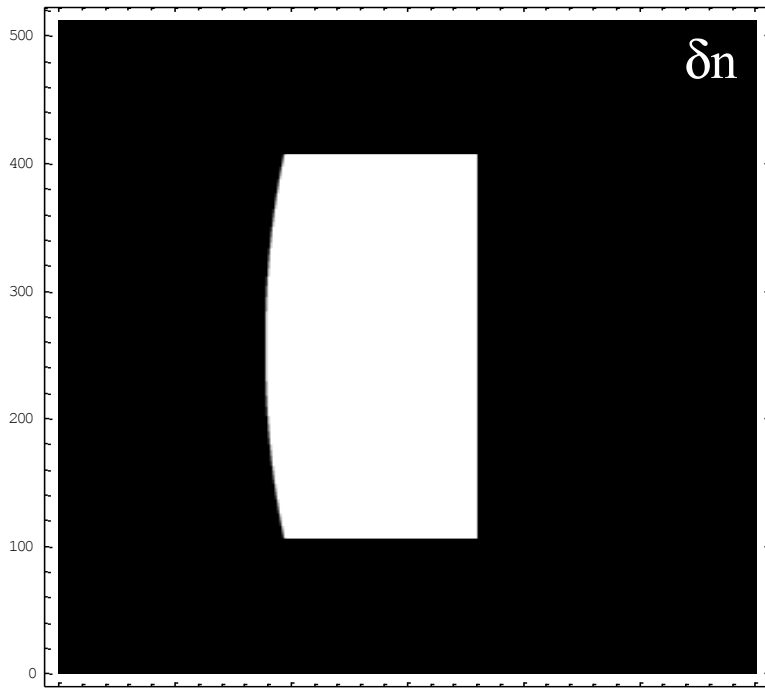
$$\delta n(x, z) = 0.01(z > 40)e^{-\left(\frac{x}{5}\right)^2}$$

$$E(x, 0) = e^{-\left(\frac{x}{30}\right)^2}$$



Curved surfaces

$$\delta n(x,z) = 0.2 \operatorname{Rect}\left(\frac{x}{300}\right) \left[x^2 + (z - 1500)^2 \leq 600^2 \text{ & } z < 1800 \right]$$

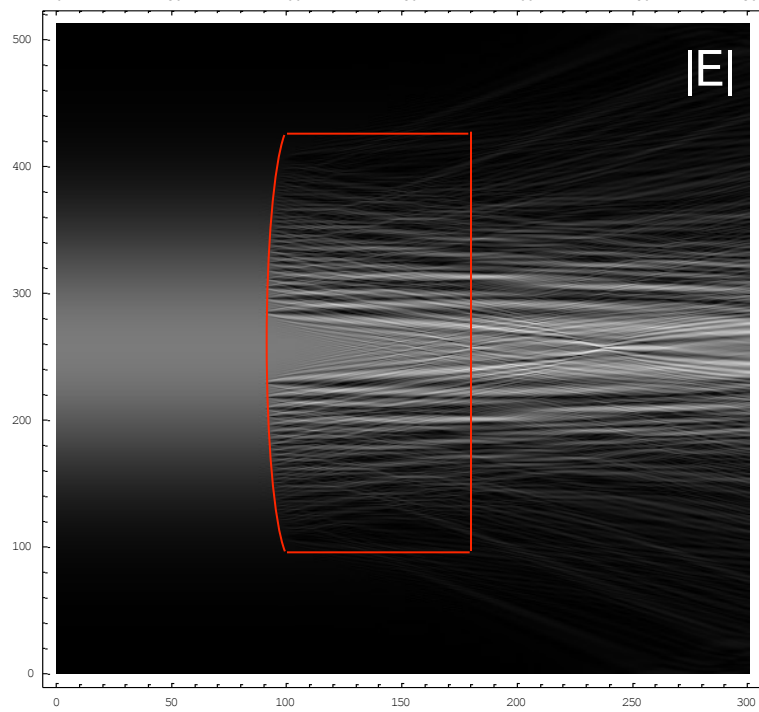


Transverse sampling
512 steps of $2 \lambda_0 = 2 \mu\text{m}$

Longitudinal sampling
300 steps of $10 \mu\text{m}$

Curved surface anti-aliased

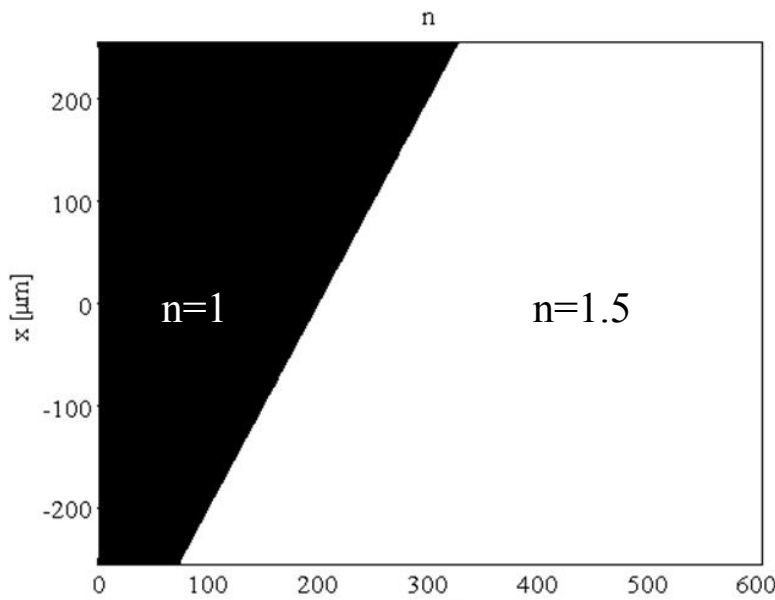
$$E(x,0) = e^{-\left(\frac{x}{200}\right)^2}$$



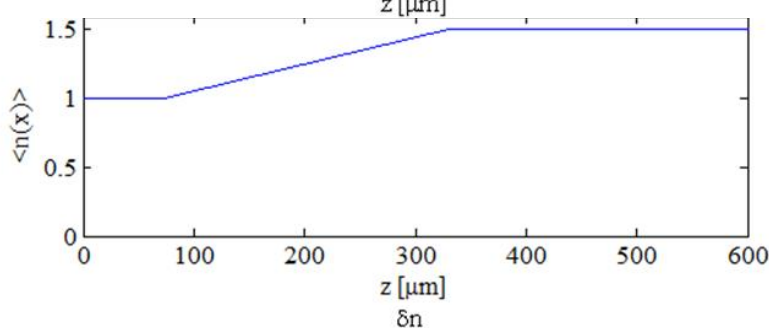
Even with averaging to reduce discontinuities, discretized surface acts as random diffraction grating

Smooth surfaces in BPM

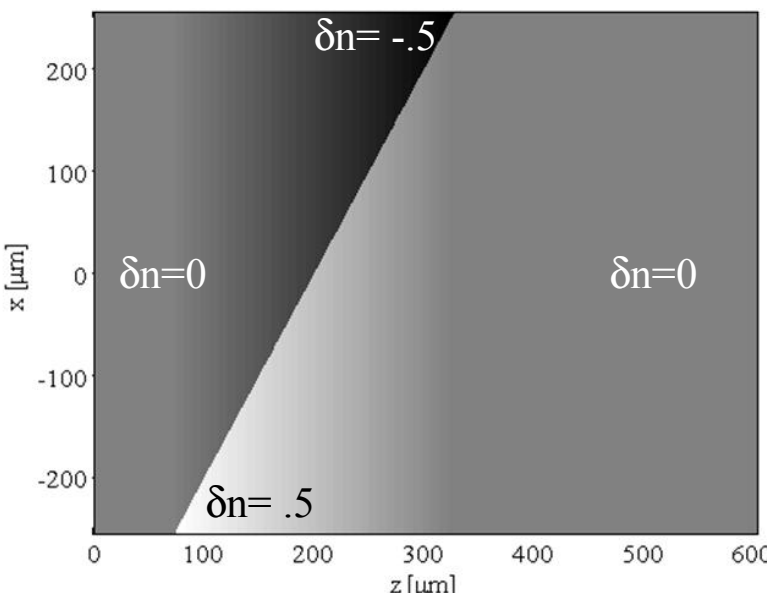
Sample problem – tilted interface



Index for an air/glass interface with a surface normal = 30°



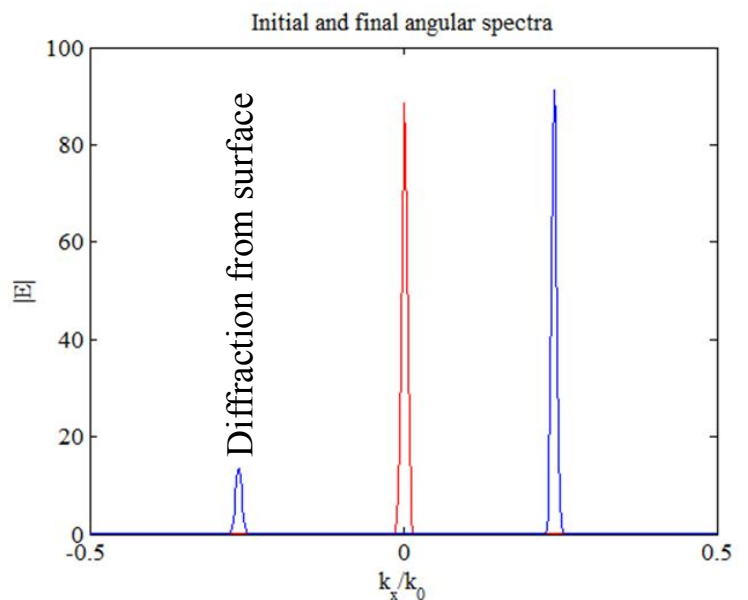
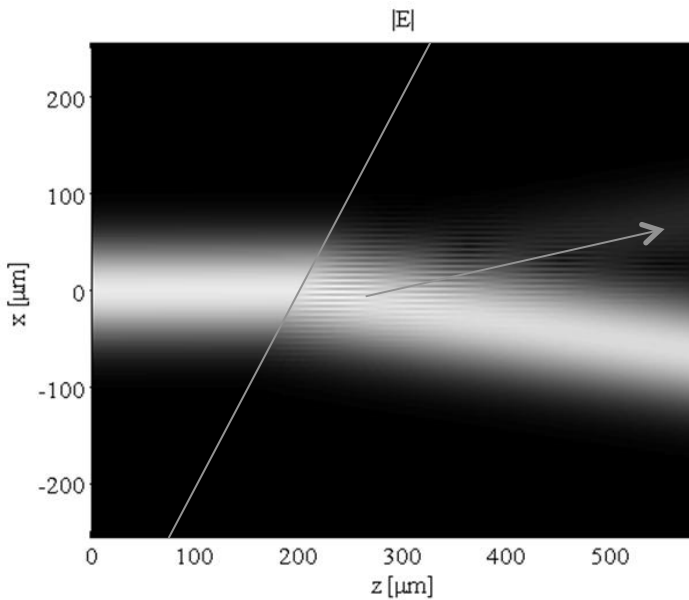
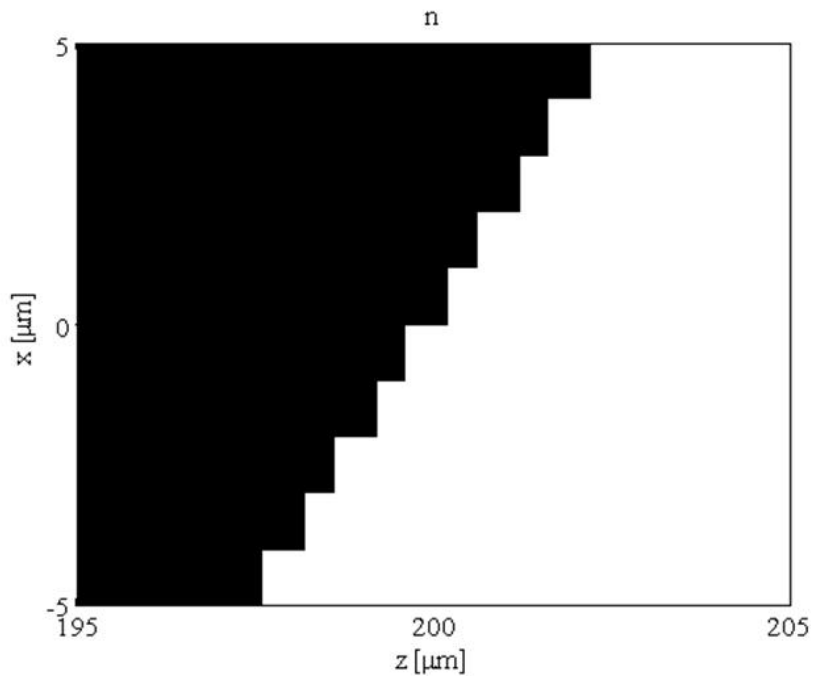
Subtract the average index at each x . The average index is used in the diffraction propagator.



The difference is the DC-free $\delta n(x)$, used in the refraction operator.

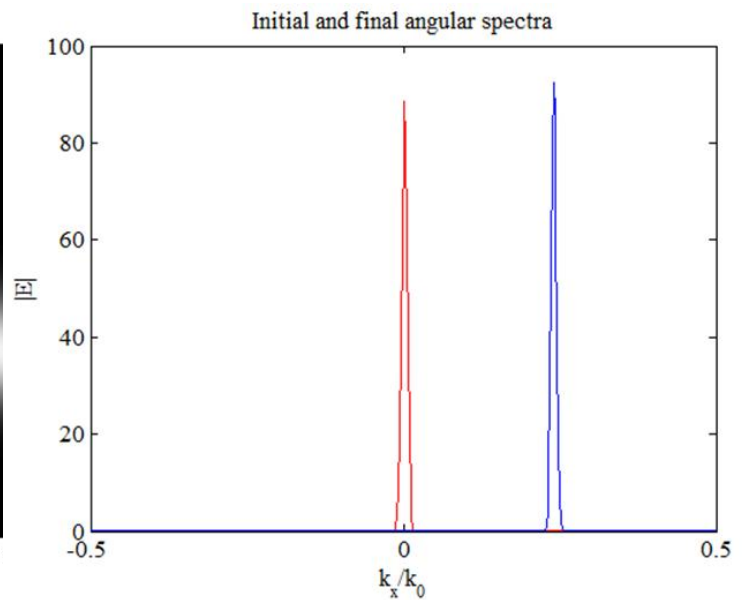
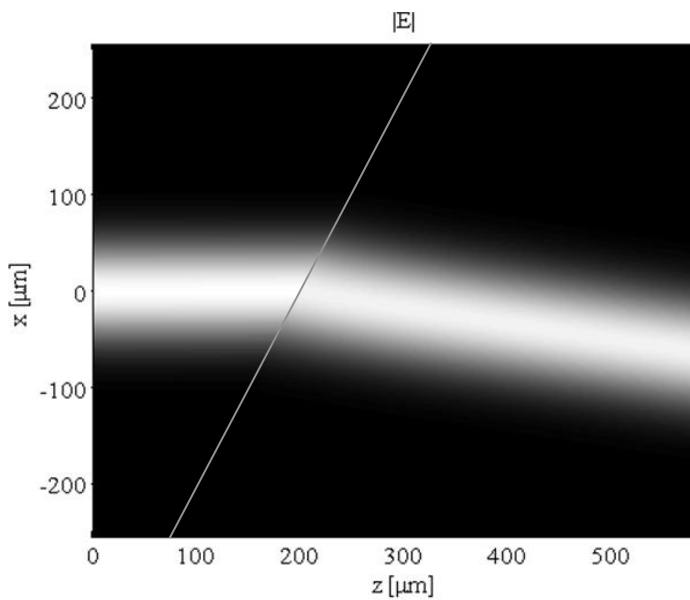
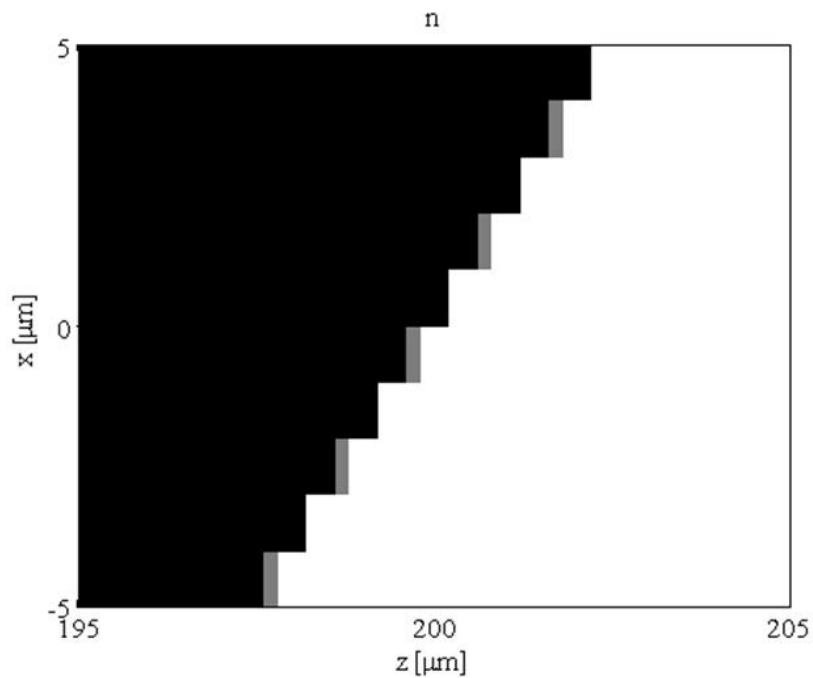
Smooth surfaces in BPM

Wrong: discretize n



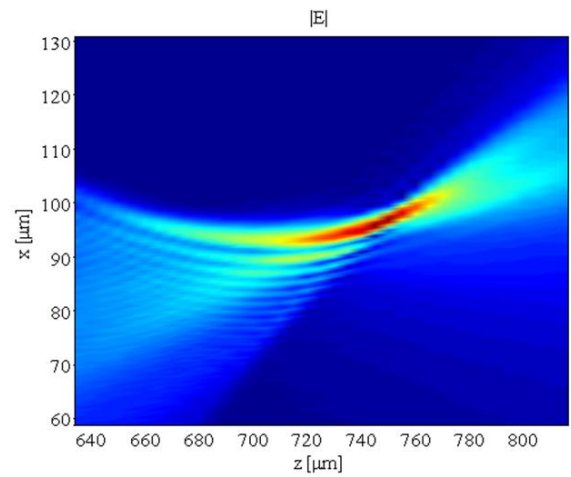
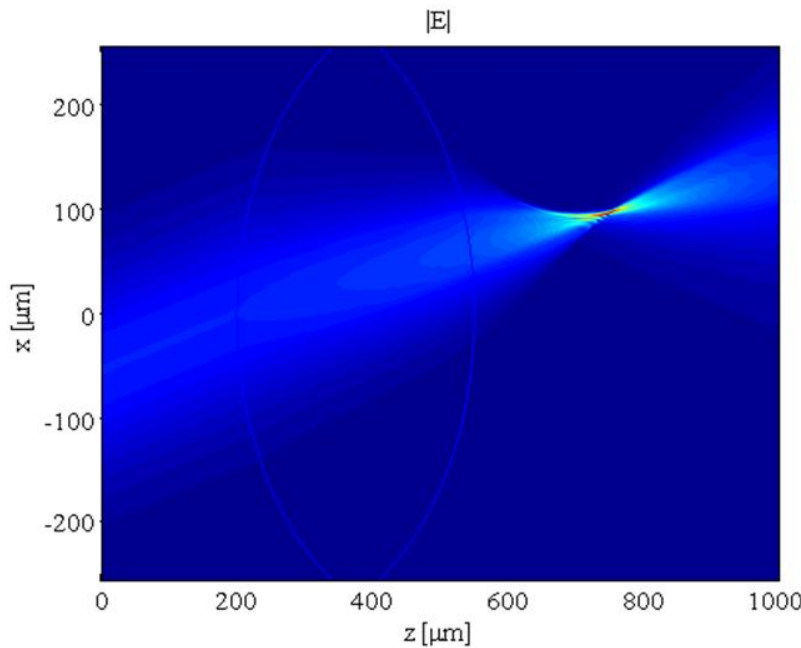
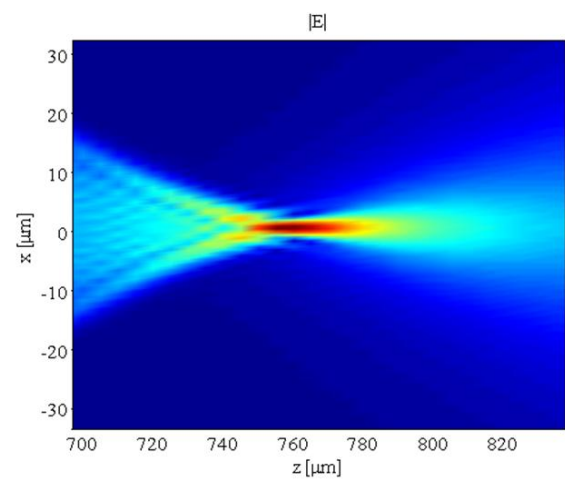
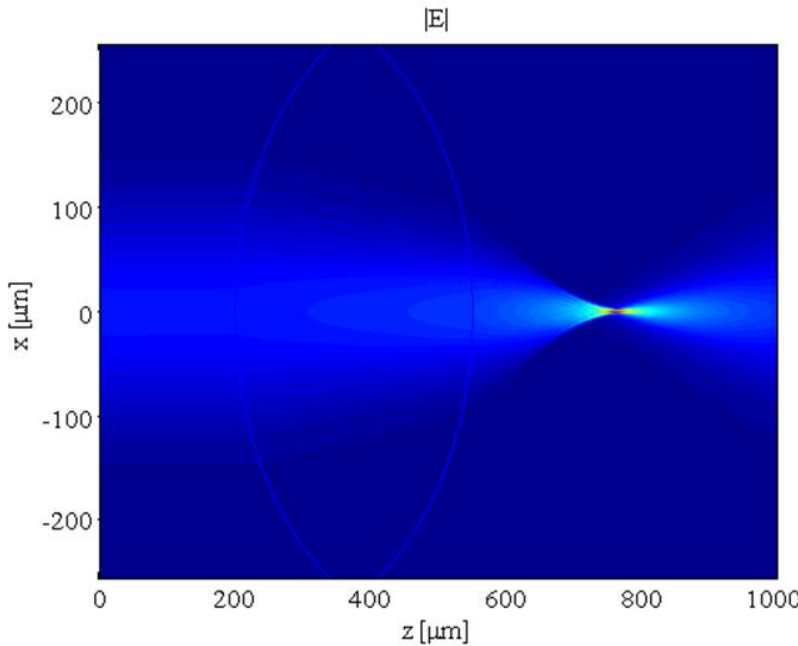
Smooth surfaces in BPM

Right: integrate n in z



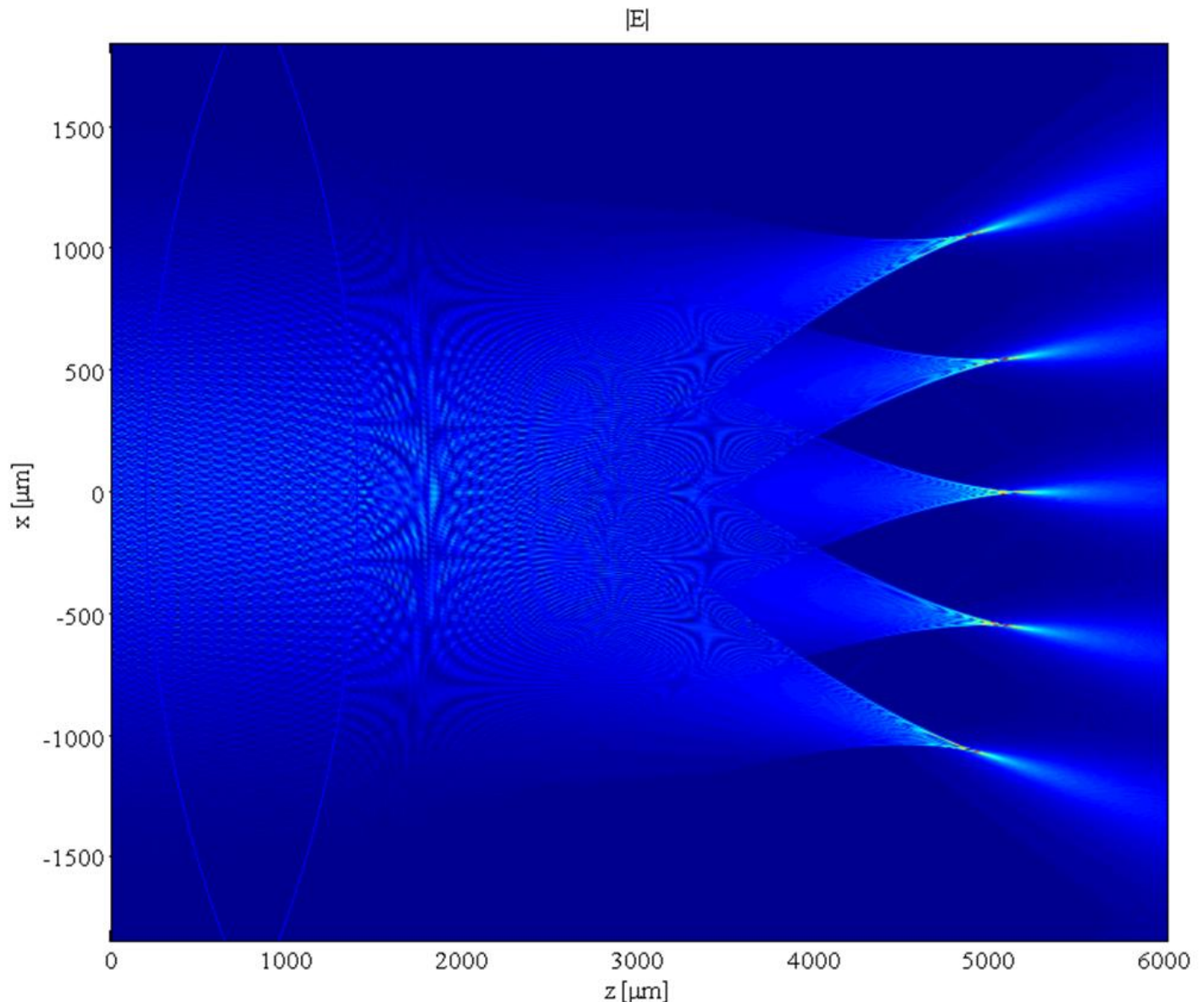
Smooth surfaces in BPM

E.g. lenses (1/2)



Smooth surfaces in BPM

E.g. lenses (2/2)

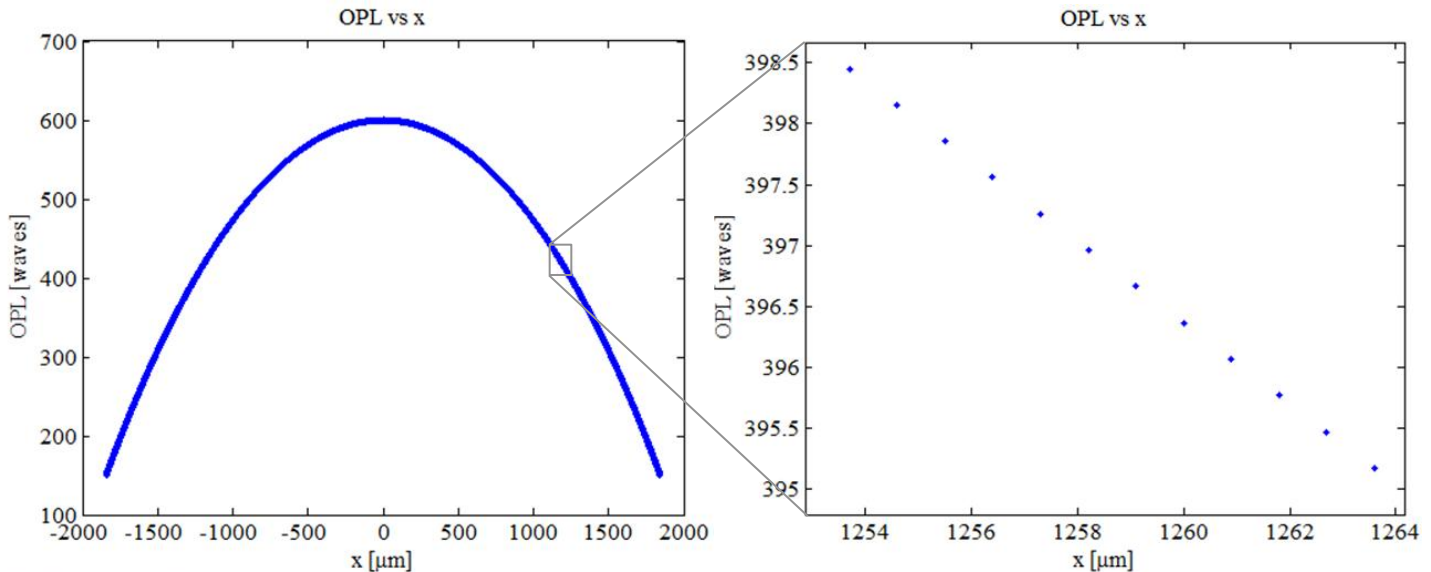


Shows expected aberration behavior including spherical, coma, and field curvature.

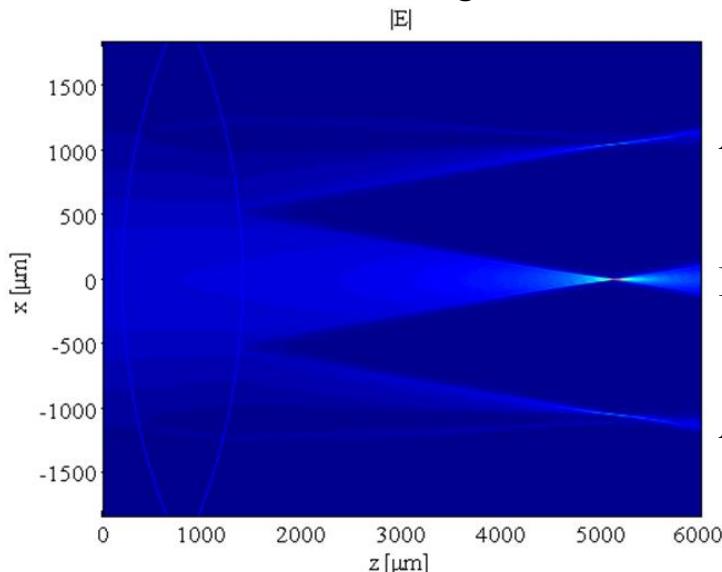
Smooth surfaces in BPM

Limitation

OPL for previous lens calculated by projection of $(n-1)$ in z.



The change in OPL between adjacent transverse samples must be $< \lambda$. If it is not, the refracted wave will suffer spatial-frequency aliasing and will propagate at an unintended angle. The Nyquist frequency is a built-in limit of transverse sampling . If the x cell size in the previous case is increased by a factor of 4, this limit is violated at the edges of the beam:



Aliasing of high angles.

Low angles within Nyquist.

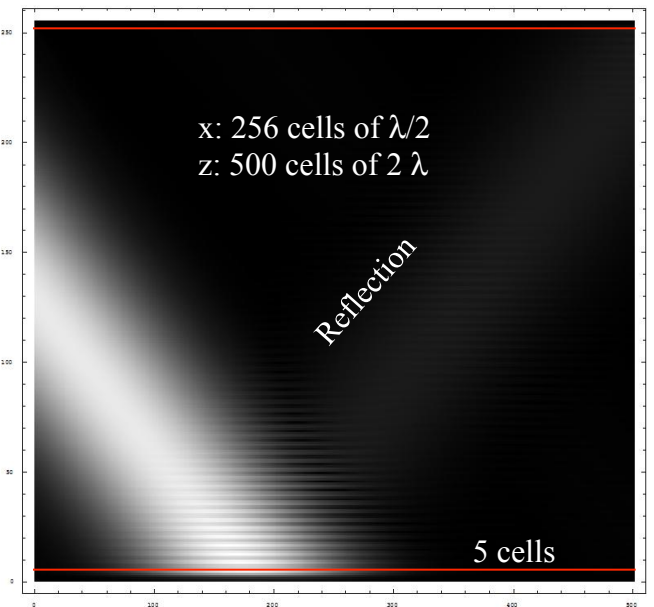
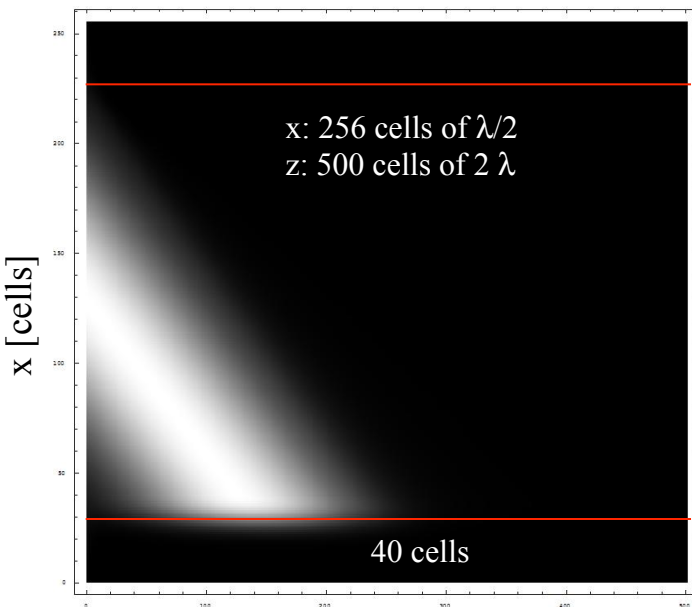
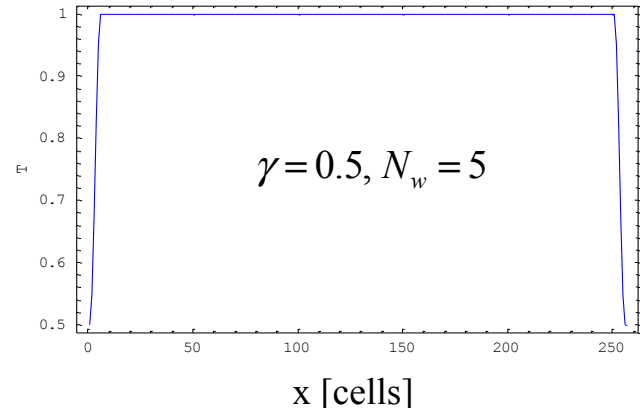
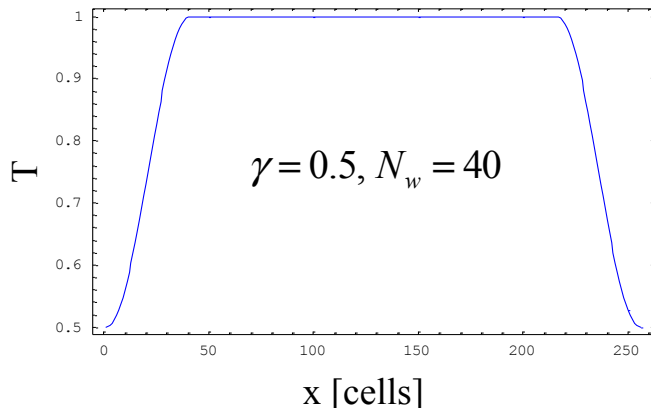
Aliasing of high angles.

- Fourier beam propagation
 - Enhancements to method
 - ABC

Absorbing boundary condition

$$T(x = m \delta x, z) = \begin{cases} \left(\frac{1-\gamma}{2}\right) \cos\left[\pi \frac{N_w + 1 - m}{N_w}\right]^\beta + \left(\frac{1+\gamma}{2}\right) & m = 1 \dots N_w \\ 1 & m = N_w + 1 \dots N_x - (N_w + 1) \\ \left(\frac{1-\gamma}{2}\right) \cos\left[\pi \frac{N_w + m - N_x}{N_w}\right]^\beta + \left(\frac{1+\gamma}{2}\right) & m = N_x - N_w \dots N_x \end{cases}$$

Adjustable parameters: γ the absorber strength, N_w the absorber width in units of δx .



$$E(x, 0) = e^{-\left(\frac{x}{30}\right)^2 - jk \sin(-10^\circ)x}$$

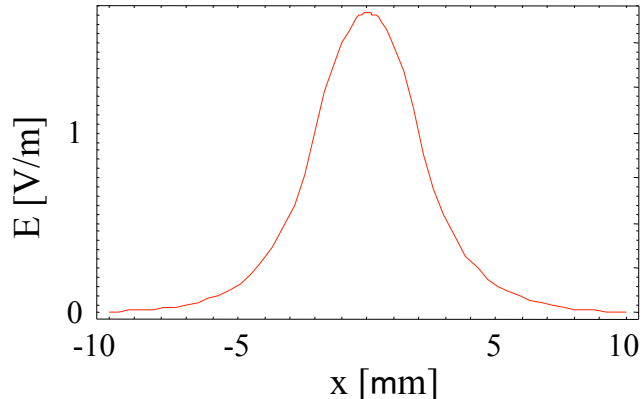
Example of conservation checking

Conservation of E in FFT BPM

Problem: Verify guided mode of step-index slab waveguide by invariance to propagation.

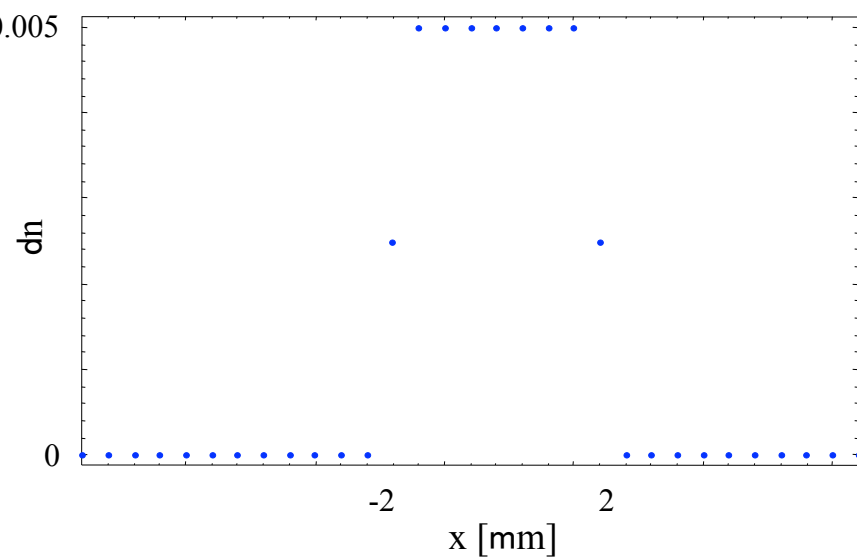
Step 1: Calculate mode with slab mode solver:

$$\begin{aligned} d &= 4 \mu\text{m} \\ \delta n &= .005 \\ n_{clad} &= 1.5 \\ \lambda &= 1.0 \mu\text{m} \end{aligned}$$

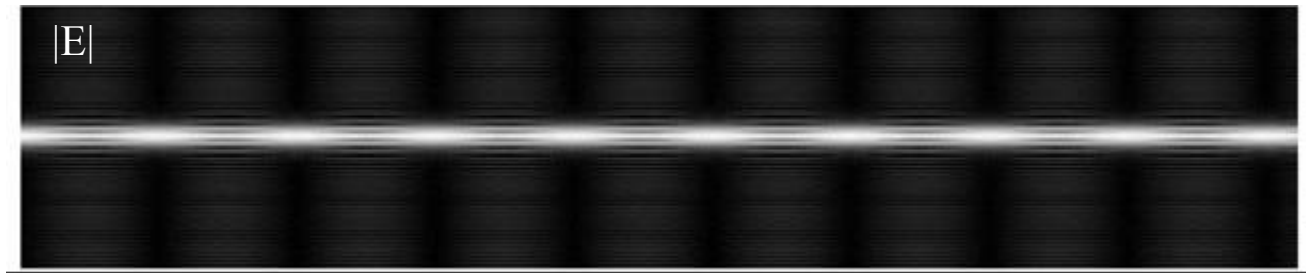


Step 2: Set dn in the BPM and launch this field

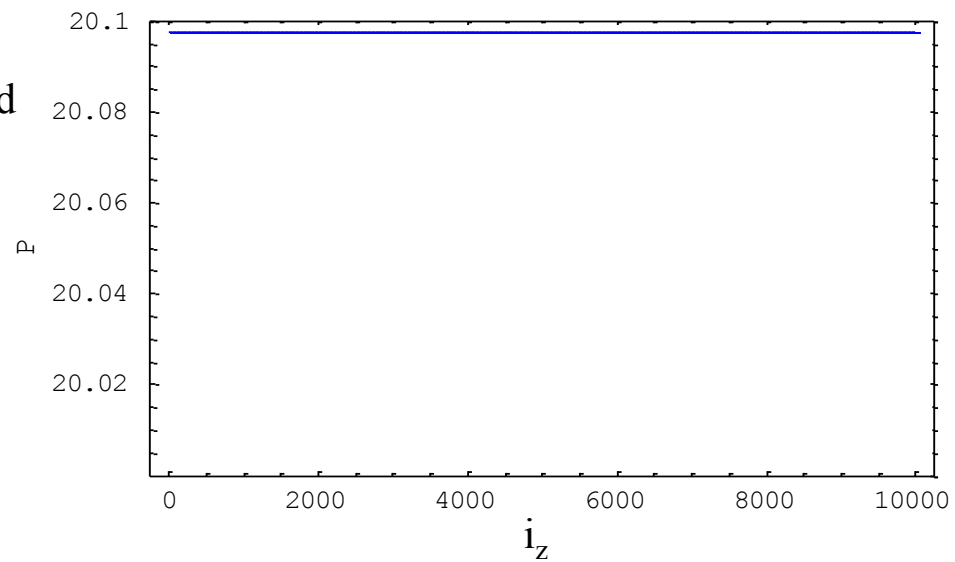
Note use of
average
index at
guide edges.



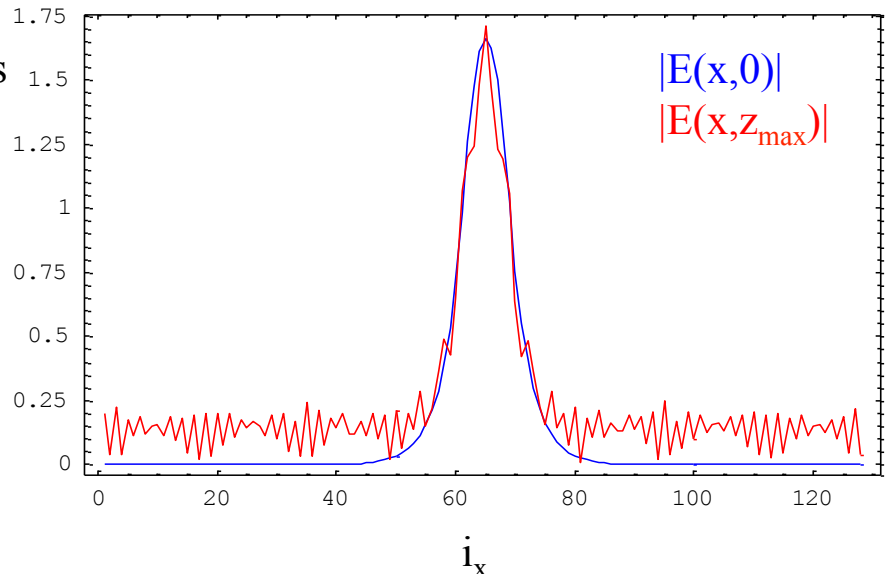
$X=128 \times 0.5 \mu\text{m}$, $Z = 10K \times 10 \mu\text{m}$
no ABC



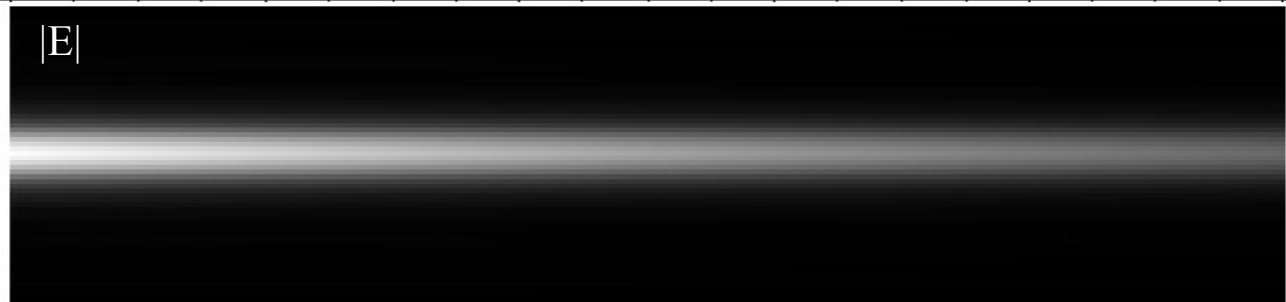
Power conserved



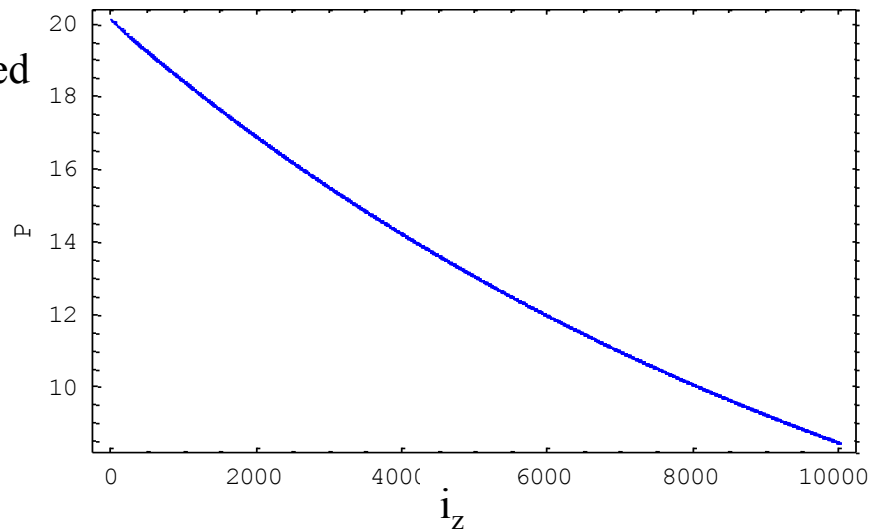
But clear reflections



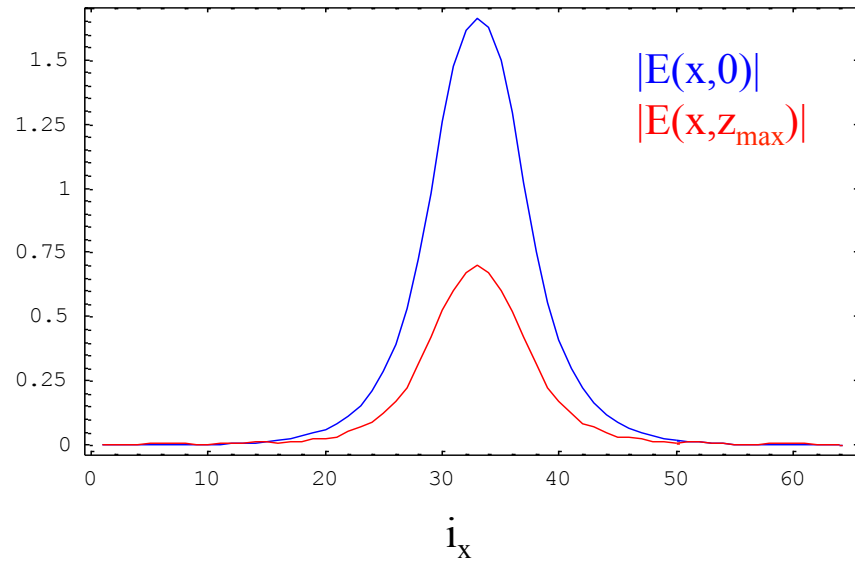
$X=128 \times 0.5 \mu\text{m}$, $Z = 10K \times 10 \mu\text{m}$
 5 cell ABC each side



Power NOT conserved



But no reflections



Largest possible Δz

When applying refraction operator, we assume that diffraction is negligible. This requires that the phase acquired by different transverse spatial frequency components be nearly the same:

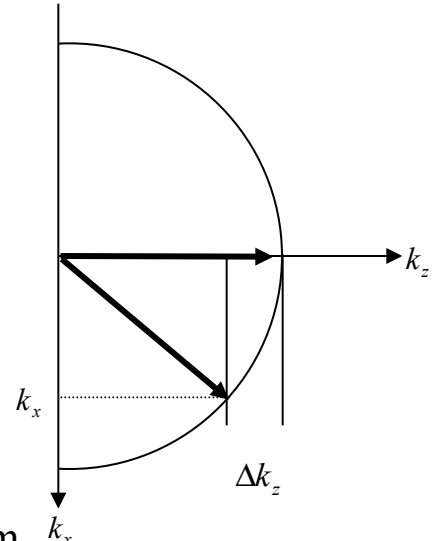
$$E(0)e^{-jkz} + E(k_x)e^{-j(k-\Delta k_z)z}$$

$$\Delta k_z \Delta z = \left[k - \sqrt{k^2 - k_x^2} \right] \Delta z \approx \frac{k^2}{2k} \Delta z = \pi$$

$$\Delta z = 2\pi \frac{k}{k_x^2}$$

For an object of finite size L

$$k_x = \frac{2\pi}{L} \quad \rightarrow \quad \Delta z_{\text{Diffraction}} = \frac{L^2}{\lambda} = 14.6 \mu\text{m}$$



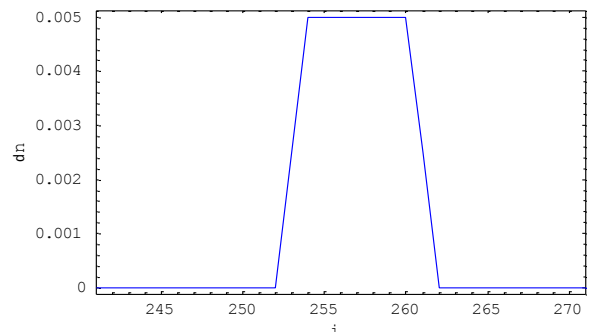
Similarly, during application of the diffraction operator we assume refraction is negligible. This requires phase at different positions be the same:

$$E(x_1)e^{-jk_0 \delta n(x_1)z} + E(x_2)e^{-jk_0 \delta n(x_2)z}$$

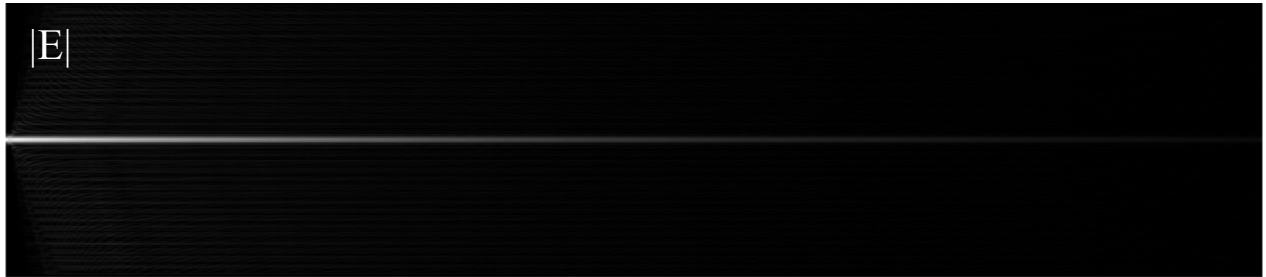
$$k_0 \Delta n \Delta z = \pi$$

$$\Delta z_{\text{Refraction}} = \frac{\lambda_0}{2\Delta n} = 100 \mu\text{m}$$

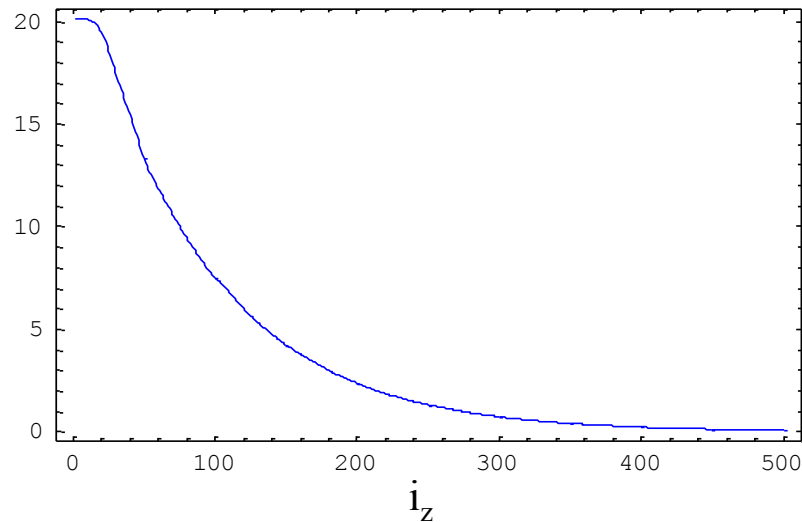
We would expect these to be the correct magnitude but too large.



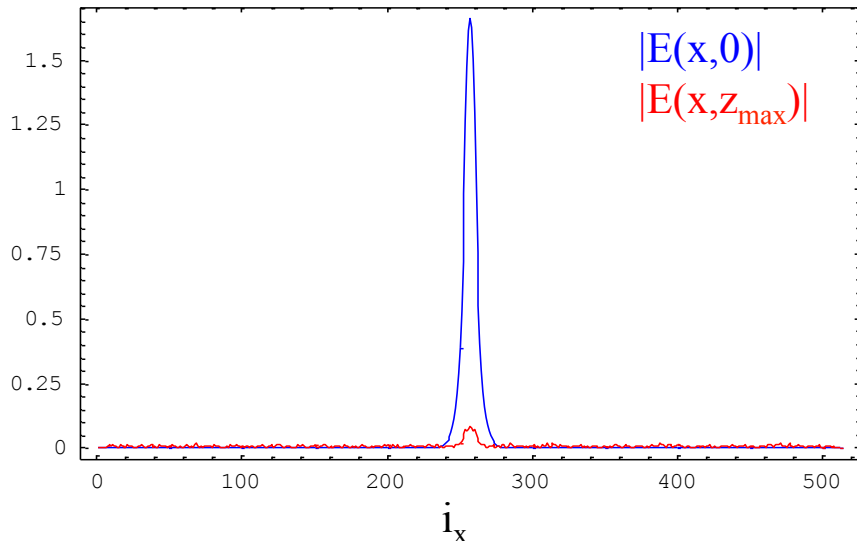
Try twice maximum Δz step $z=500$ steps of $2 \times 14.6 \mu\text{m}$



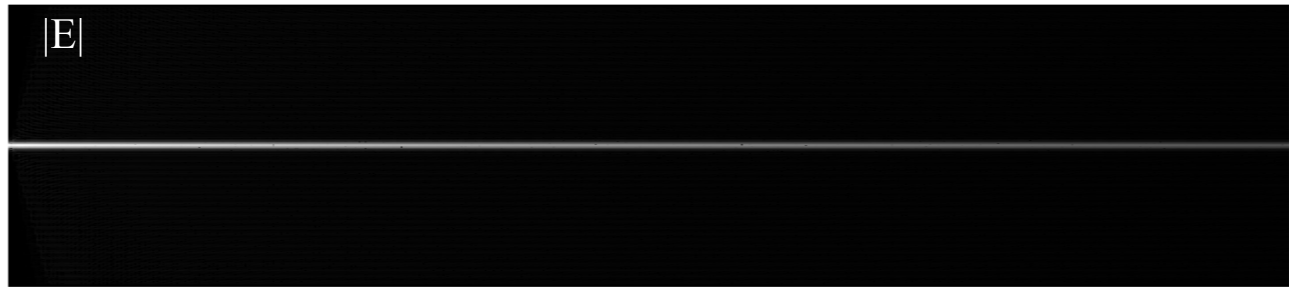
Power really not conserved! Thus the extra-long step in z is breaking the guiding, allowing light to leak and be absorbed by the ABC.



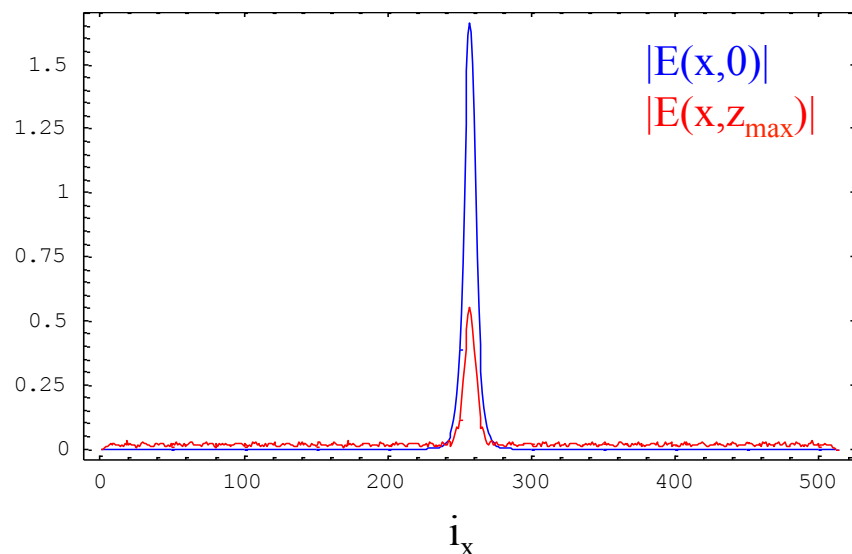
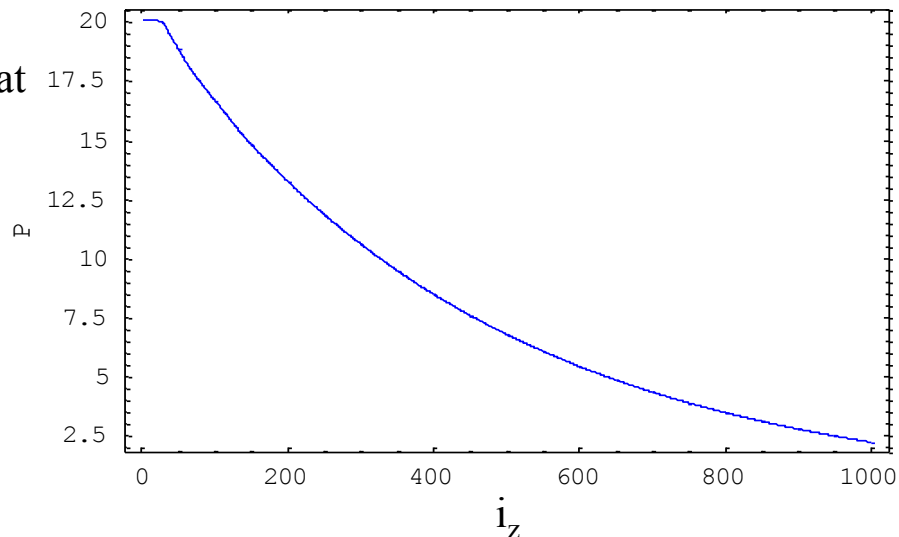
Almost nothing left at end



Try maximum Δz step
 $z=1000$ steps of 14.6 mm

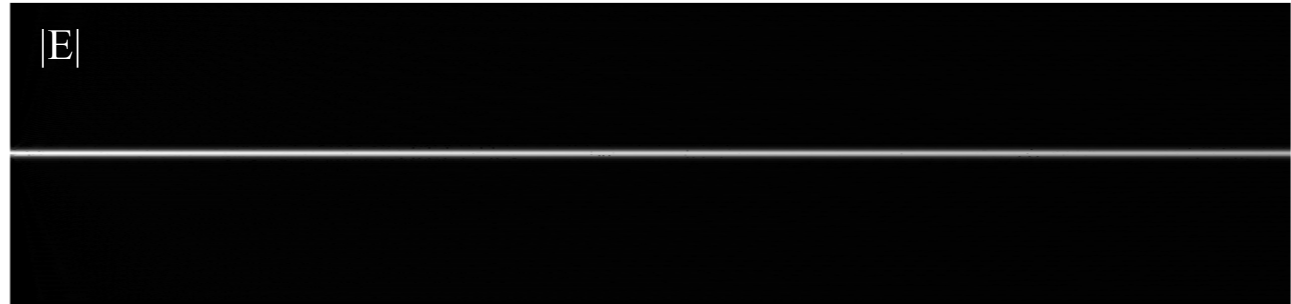


Better but not great

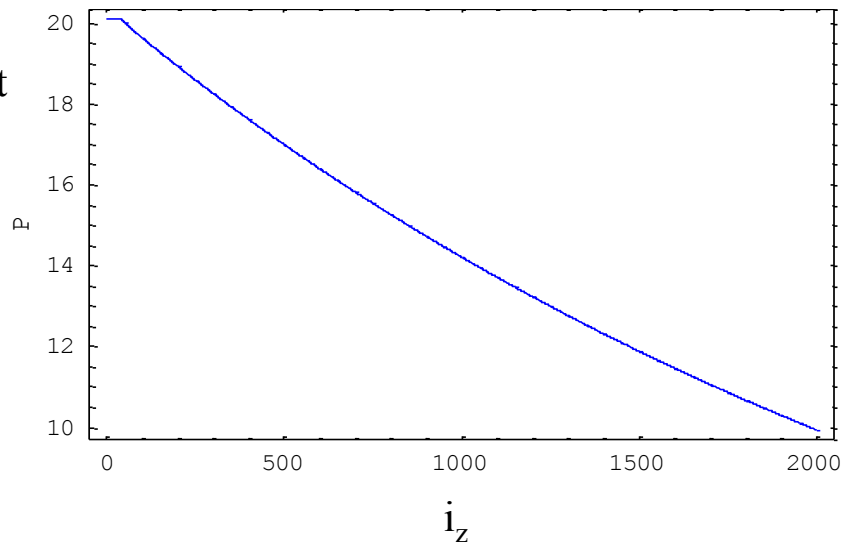


Half maximum Δz step

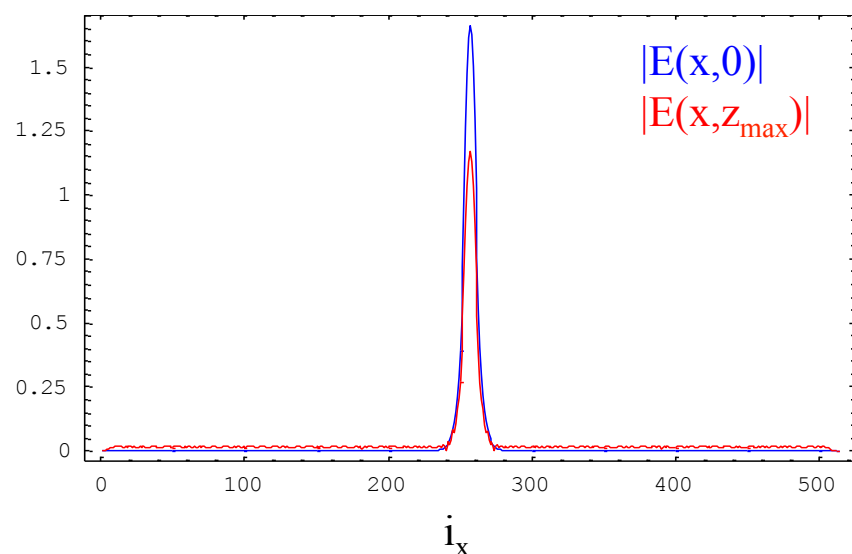
$z=2000$ steps of $14.6/2 \mu\text{m}$



Only $\frac{1}{2}$ of power lost



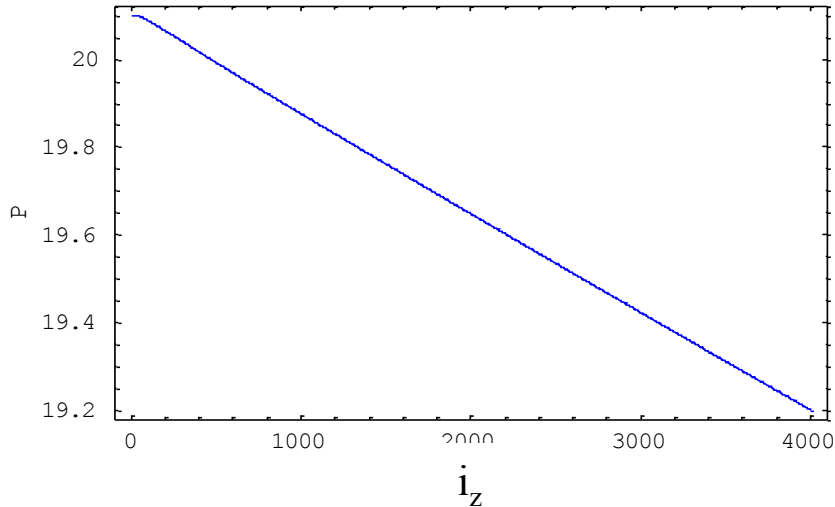
Field at end of
guide beginning to
look like launch



1/4 maximum Δz step z=4000 steps of 14.6/4 μm



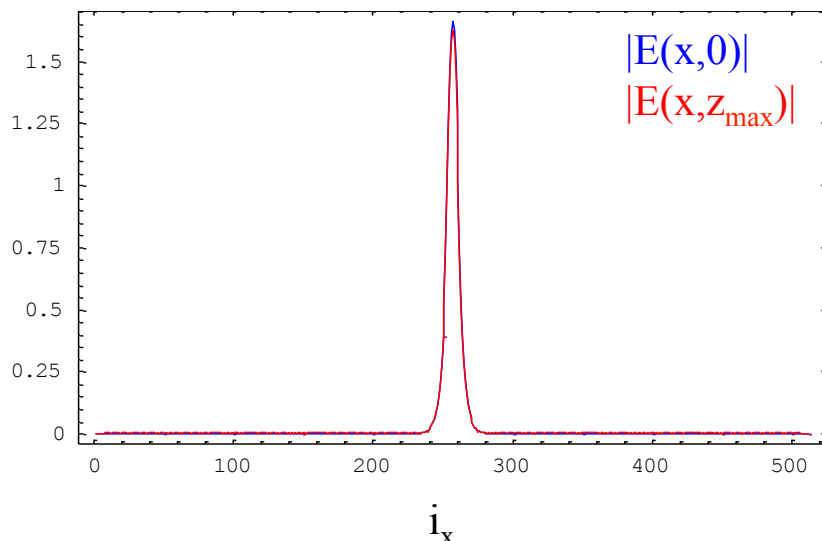
Pretty good. Only 4.5% of power lost



Electric fields at entry and exit overlap.

Therefore

$$\Delta z \leq \frac{1}{4} \min\left(\frac{\lambda_0}{2\Delta n}, \frac{L^2}{\lambda}\right)$$



Acoustooptics (1/3)

Typically grating is quite weak so can approximate the refraction step as

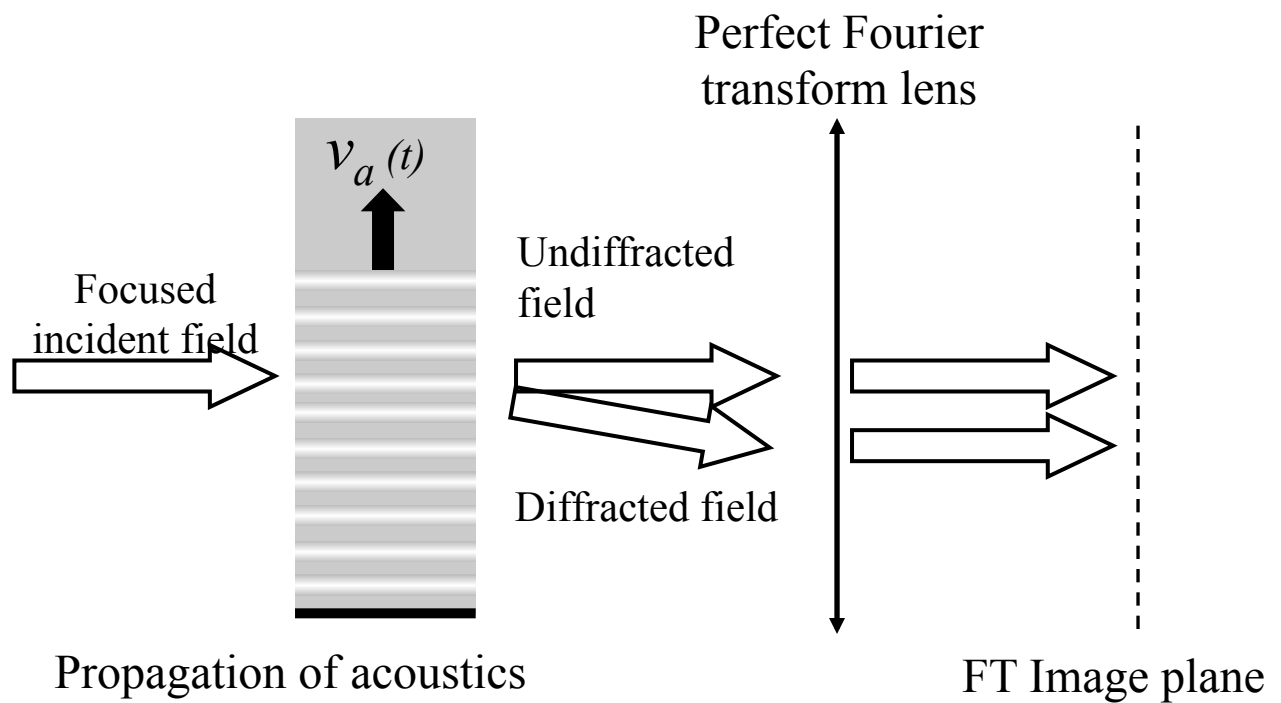
$$\begin{aligned}
e^{-jk_0 \delta n \Delta z} &\approx 1 - j k_0 \delta n \Delta z \\
&= 1 - j k_0 \Delta z C \sin(\Omega t - K x) \\
&= 1 - k_0 \Delta z \frac{C}{2} \left(e^{j(\Omega \vec{t} - K \vec{x})} - e^{-j(\Omega \vec{t} - K \vec{x})} \right)
\end{aligned}$$

Jarem and Banerjee present an algorithm that simultaneously simulates both the positive and negative side-bands using shifts in the Fourier space to represent the grating, but there's a problem with this. Each side band is positive or negative Doppler shifted, which we can not simulate in a one single-frequency simulation. Thus the two terms will appear to interfere, but should not.

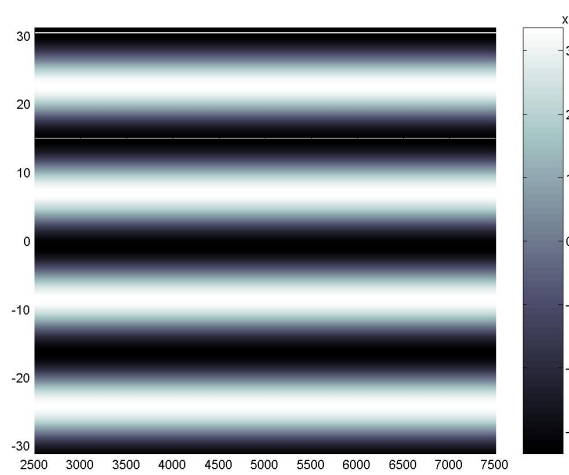
Solution 1: Ignore problem but examine fields only where diffraction off of individual side-bands don't overlap

Solution 2: Only simulate one side-band since Bragg matching typically makes only one important.

Acoustooptics (2/3)

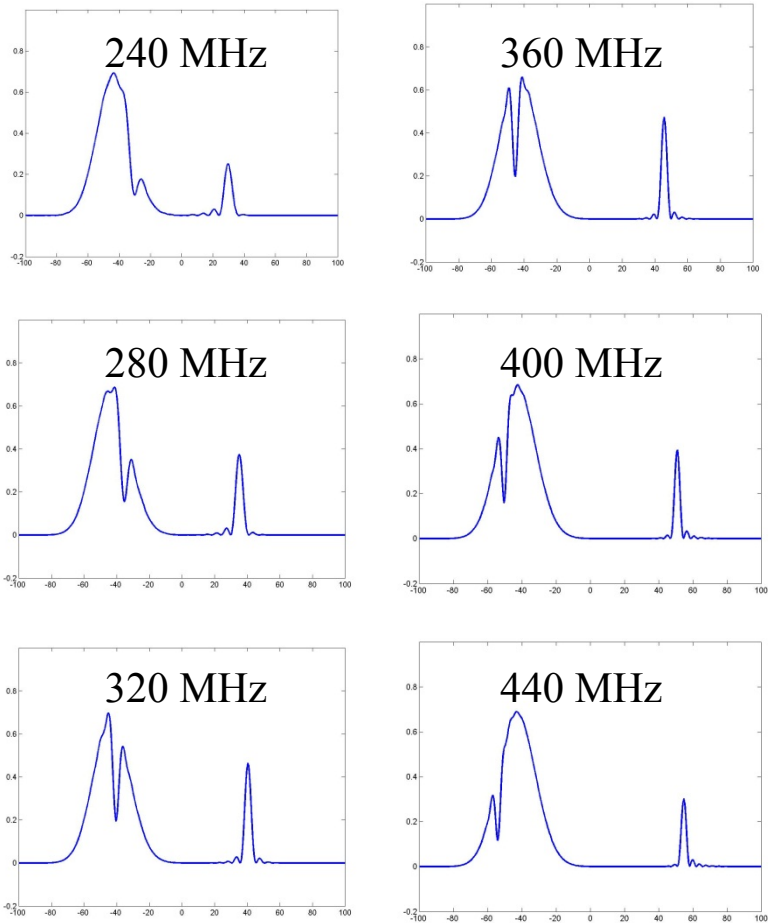


Portion of index structure at one time instant

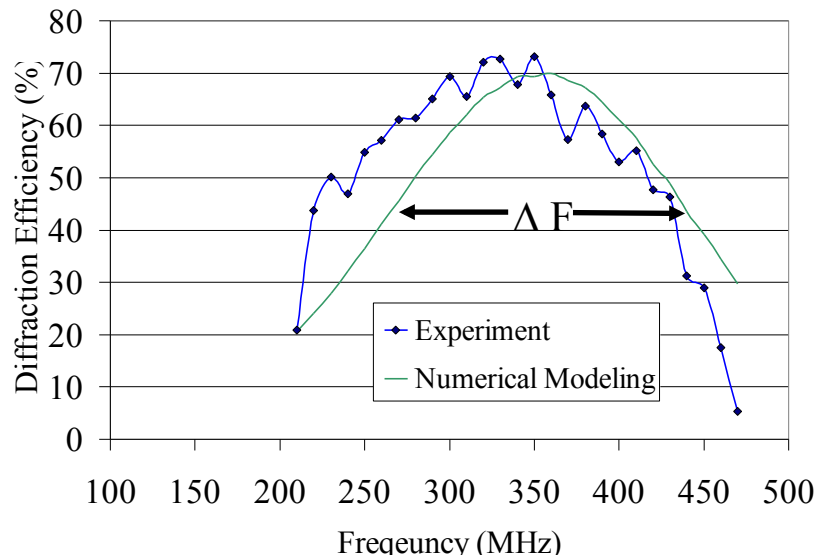


Acoustooptics (3/3)

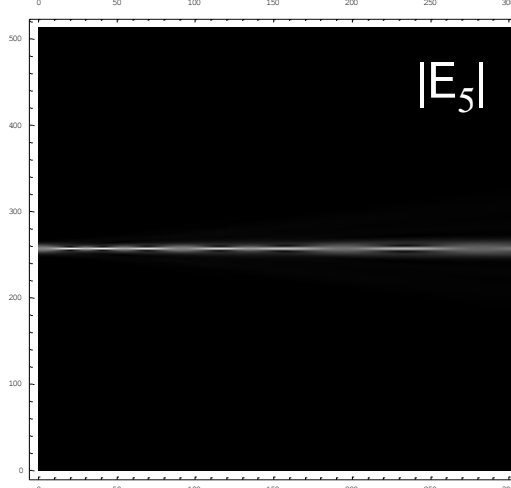
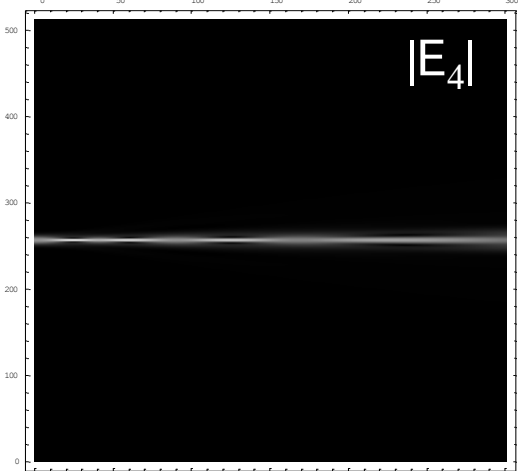
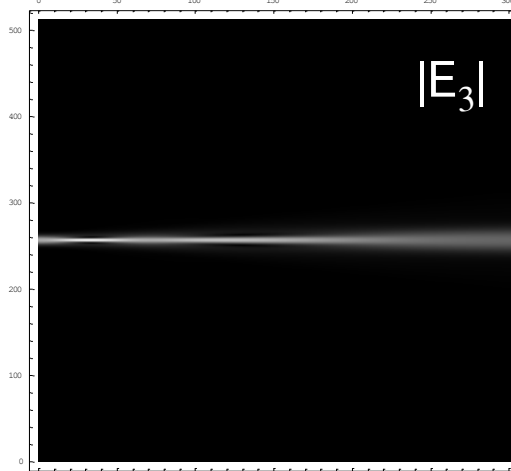
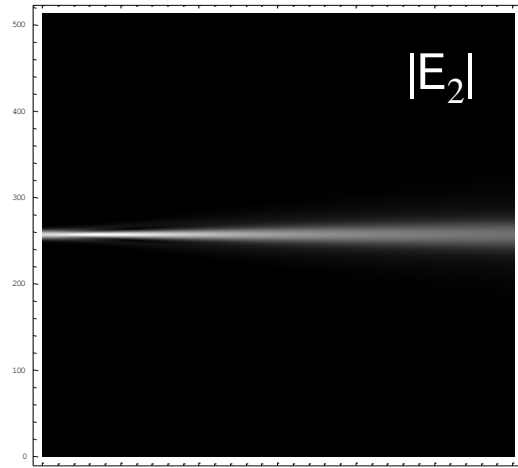
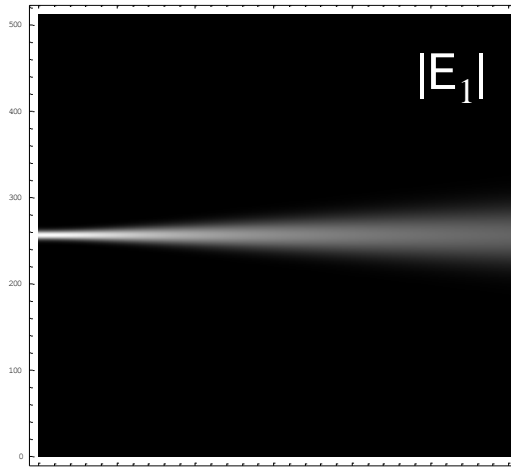
- “Hole” carved in angular spectrum of incident beam.
- Bragg matching causes “hole” to change in location
- Efficiency of diffraction depends on distribution in K-space



- Matches well to experiment
- Offset likely due to small rotation of crystal around acoustic propagation direction
- Accurately predicts bandwidth of device



Integrating nonlinearity e.g. photopolymer



$$\delta n(x, z) = \int 10^{-3} |E|^2 dt$$

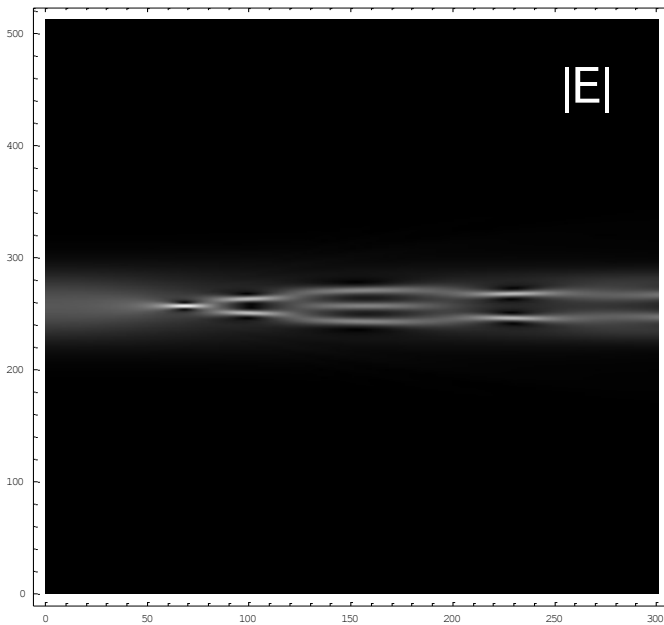
Filament forms.
No saturation in this model, which might stabilize

Kerr nonlinearities

In the mid 80's, amplifiers on the Nova laser had the habit of developing tiny pinholes in the direction of propagation. This was identified as nonlinear focusing. Mike Feit and Joe Fleck successfully predicted the formation of high-intensity filaments using *nonparaxial* beam propagation. Conservation of energy in the simulation is essential (several early works used a difference scheme that gave nonphysical results due to numerical nonlinear absorption).

Simple scalar, instantaneous χ^3 nonlinearity

$$n(E) = n_0 + n_2 |E|^2$$



Transverse sampling
512 steps of $1 \lambda_0 = 1 \mu\text{m}$

Longitudinal sampling
300 steps of $10 \mu\text{m}$

$$\delta n(x, z) = 10^{-3} |E|^2$$

$$E(x, 0) = e^{-\left(\frac{x}{30}\right)^2}$$

Solitons

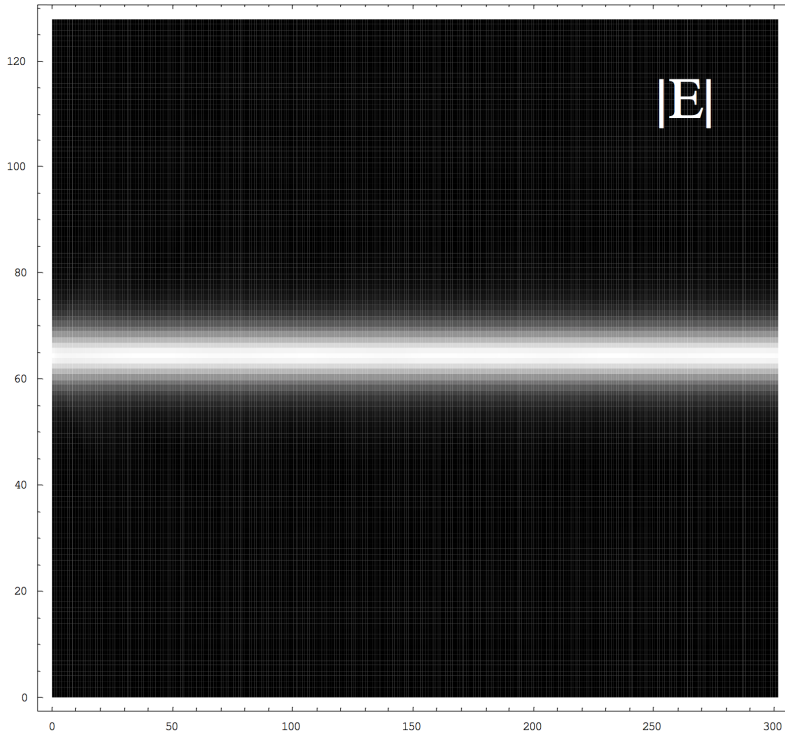
Substitute the equation for n into the wave equation to get the nonlinear Schrodinger equation.

$$\frac{\partial}{\partial z} \mathcal{E} = \frac{1}{2jk} \nabla_{\perp}^2 \mathcal{E} - jk_0 n_2 |\mathbf{E}|^2 \mathcal{E} \quad k \equiv k_0 n_0$$

In one dimension this has a stable solution:

$$\mathcal{E}(x) = \sqrt{\frac{\kappa}{n_2 k_0}} \operatorname{sech}\left(x \sqrt{\kappa k}\right)$$

where κ is a free parameter



Transverse sampling
512 steps of $\lambda_0 / n_0 = 1/1.5 \mu\text{m}$

Longitudinal sampling
300 steps of $10 \mu\text{m}$

$$\delta n(x, z) = 10^{-3} |\mathbf{E}|^2$$

$$\kappa = 1/50 \left[\frac{1}{\mu\text{m}} \right]$$

Solitons in multiple dimensions (x,y,t)

Write the permittivity as a sum of frequency dependent dispersive linear and instantaneous nondispersive nonlinear parts

$$\begin{aligned}\epsilon &= \epsilon_L(\omega) + \epsilon_{NL}(E) \\ &= \epsilon_L + (\omega - \omega_0) \frac{\partial \epsilon_L}{\partial \omega} \Big|_{\omega_0} + \frac{1}{2}(\omega - \omega_0)^2 \frac{\partial^2 \epsilon_L}{\partial \omega^2} \Big|_{\omega_0} + \chi^{(3)} |E|^2\end{aligned}$$

or, taking $\epsilon = n^2 = (n_0 + \delta n)^2 \approx n_0^2 + 2 n_0 \delta n$

$$n = n_0 + \frac{1}{2n_0}(\omega - \omega_0) \frac{\partial \epsilon_L}{\partial \omega} \Big|_{\omega_0} + \frac{1}{2n_0} \frac{1}{2}(\omega - \omega_0)^2 \frac{\partial^2 \epsilon_L}{\partial \omega^2} \Big|_{\omega_0} + n_2 |E|^2$$

Shift into the GV coordinate system and scale the field and coordinates

$$\begin{aligned}1/V_g &\equiv \frac{\partial k}{\partial \omega} \Big|_{\omega_0} = \left(\frac{n_0}{c} + \frac{\omega_0}{c} \frac{\partial n_0}{\partial \omega} \right) = \frac{1}{n_0 c} \left(\epsilon_L + \frac{\omega_0}{2} \frac{\partial \epsilon_L}{\partial \omega} \right) \\ D &\equiv -\frac{\partial^2 k}{\partial \omega^2} \Big|_{\omega_0} = \frac{1}{\omega_0 n_0 c} \left(\epsilon_L + 2\omega_0 \frac{\partial \epsilon_L}{\partial \omega} + \frac{\omega_0^2}{2} \frac{\partial^2 \epsilon_L}{\partial \omega^2} \right)\end{aligned}$$

$$\tau = (t - z/V_g)(k_0/D)^{1/2}$$

$$u = (n_2/n_0)^{1/2} \mathcal{E}$$

$$(\xi, \eta, \zeta) = (k_0 x, k_0 y, k_0 z)$$

to give the unitless, 3+1 dimensional nonlinear Schrodinger equation (NLS)

$$-j \frac{\partial u}{\partial \zeta} + \frac{1}{2} \nabla_{\xi \eta \tau}^2 u + |u|^2 u = 0$$

Eigen-solutions of NLS

Assume a stable (eigen) solution that propagates only with a change of phase:

$$u = U(\rho) \exp(j\beta\zeta) \quad \rho = \sqrt{\xi^2 + \eta^2 + \tau^2}$$

which reduces the d -dimensional NLS to an ordinary DE in the radial coordinate, r

$$\frac{1}{2} \left[\frac{\partial^2}{\partial \rho^2} + \frac{d-1}{\rho} \frac{\partial}{\partial \rho} \right] U - \beta U + U^3 = 0$$

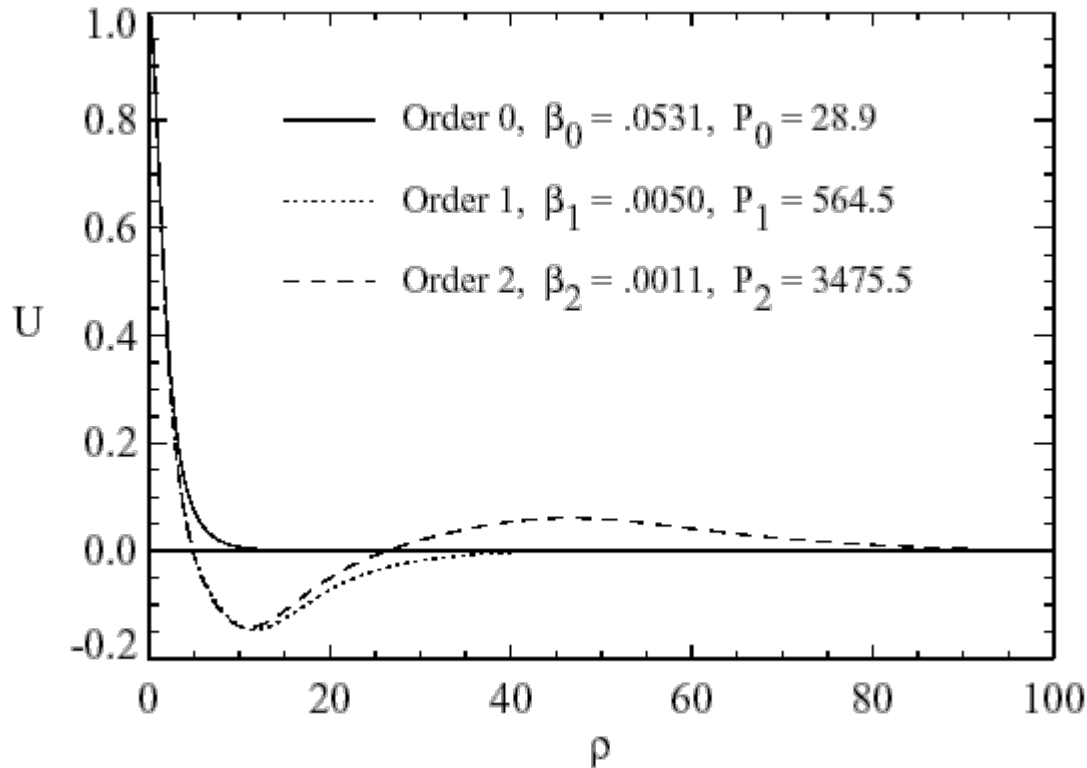
$$\tilde{U}(\rho) = aU(a\rho)$$

We can deduce a scaling relationship from this equation

$$\tilde{P} = a^{2-d} P$$

$$\tilde{\beta} = a^2 \beta$$

Solutions for $d=3$, $a=1$:



Solution in various coordinate systems

To solve the diffraction portion of the $d+1$ dimensional NLS, we need to express the field u as a sum of the eigenfunctions of the Laplacian:

$$\nabla^2 \Gamma(\vec{\rho}, \vec{\kappa}) = -k^2 \Gamma(\vec{\rho}, \vec{\kappa})$$

Since Γ is an orthogonal, complete basis in d dimensions, we can write the transform pair:

$$\begin{aligned} u(\vec{\rho}) &= \int \int \int U(\vec{\kappa}) \Gamma(\vec{\rho}, \vec{\kappa}) d^3 \kappa \\ U(\vec{\kappa}) &= \int \int \int u(\vec{\rho}) \Gamma^*(\vec{\rho}, \vec{\kappa}) d^3 \rho \end{aligned}$$

In rectangular, cylindrical, and spherical coordinates, Γ has the following forms

$$\text{Rectangular : } \Gamma(\vec{\rho}, \vec{\kappa}) = \begin{cases} e^{+j(\kappa_x x + \kappa_y y + \kappa_z z)} & k^2 = \kappa_x^2 + \kappa_y^2 + \kappa_z^2 \\ e^{-j(\kappa_x x + \kappa_y y + \kappa_z z)} \end{cases}$$

$$\text{Cylindrical : } \Gamma(\vec{\rho}, \vec{\kappa}) = \begin{cases} J_m(\kappa_\rho \rho) e^{-j(m\phi + \kappa_z z)} & k^2 = \kappa_\rho^2 + \kappa_z^2; \\ Y_m(\kappa_\rho \rho) e^{-j(m\phi + \kappa_z z)} & m = \dots -1, 0, 1 \dots \end{cases}$$

$$\text{Spherical : } \Gamma(\vec{\rho}, \vec{\kappa}) = \begin{cases} j_l(\kappa_\rho \rho) Y_l^m(\theta, \phi) & k^2 = \kappa_\rho^2, l = 0, 1, 2 \dots; \\ y_l(\kappa_\rho \rho) Y_l^m(\theta, \phi) & m = -l, \dots, l \end{cases}$$

where J_m and Y_m are Bessel functions, j_l and y_l are the spherical Bessel functions and Y_l^m is the spherical harmonic

Soliton stability by BPM in spherical coordinates

Solitons are stable to propagation when $dP / d\beta > 0$. Using the scaling relationship, we can find

$$\frac{dP}{d\beta} = \left(1 - \frac{d}{2}\right) \left(\frac{\beta}{\beta_{d0}}\right)^{-d/2} \frac{P_{d0}}{\beta_{d0}} \quad \begin{cases} > 0 & \text{if } d = 1 \\ = 0 & \text{if } d = 2 \\ < 0 & \text{if } d = 3 \end{cases} \quad \begin{matrix} \text{Stable} \\ \text{Marginally stable} \\ \text{Unstable} \end{matrix}$$

To verify this prediction, let us assume only a radial dependence to the field u and propagate in this reduced spherical coordinate system. The eigenfunctions of the Laplacian reduce to:

$$j_0(\kappa_\rho \rho) = e^{\pm j\kappa_\rho \rho} / \rho \quad (m = l = 0)$$

The transformation into the radial k-space can then be written with Fourier transforms:

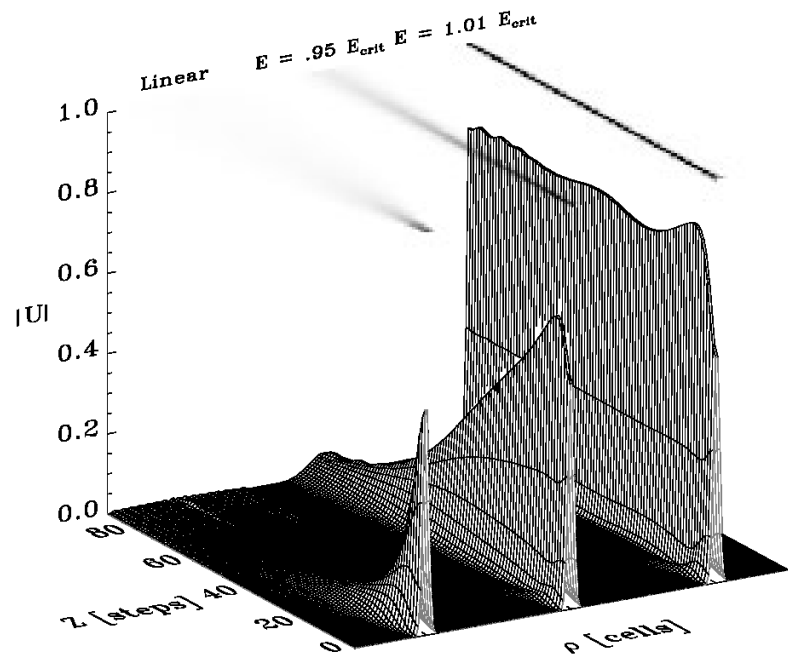
$$\begin{aligned} U(\kappa_\rho) &= \iiint u(\rho) \frac{e^{-j\kappa_\rho \rho}}{\rho} d^3 \rho && \text{Forward transform} \\ &= 4\pi \int u(\rho) \rho e^{-j\kappa_\rho \rho} d\rho \\ &= 4\pi \mathcal{F}[u(\rho)\rho] \end{aligned}$$

$$\begin{aligned} u(\rho) &= \iiint U(\kappa_\rho) \frac{e^{j\kappa_\rho \rho}}{\rho} d^3 \kappa && \text{Reverse transform} \\ &= \int \sum_l \sum_m U(\kappa_\rho) \frac{e^{j\kappa_\rho \rho}}{\rho} d\kappa_\rho \\ &= \frac{1}{\rho} \int U(\kappa_\rho) e^{j\kappa_\rho \rho} d\kappa_\rho \\ &= \frac{1}{\rho} \mathcal{F}^{-1}[U(\kappa_\rho)] \end{aligned}$$

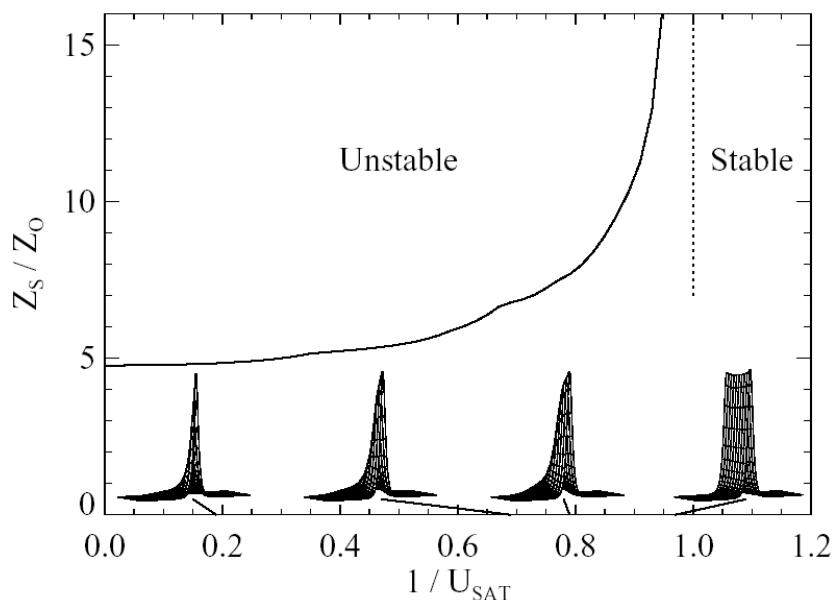
Results of radial-spherical BPM with saturating n_2

Replace $n_2 |E|^2$ with $n_2 |E|^2 / (1 + |E|^2 / E_{\text{sat}}^2)$. Previous stability test now predicts stable 3+1 light-bullets when $E(0) \geq E_{\text{sat}}$

Three radial-spherical BPM results for linear medium, $E(0) = 95\% E_{\text{sat}}$ and $E(0) = 1.01 E_{\text{sat}}$



Distance of stable propagation vs strength of saturation



Vector nonlinear propagation

As usual, write the linear material properties for the ordinary and extra-ordinary polarization

$$\begin{aligned}\epsilon_o(\omega) &= \epsilon_{oL} + (\omega - \omega_0) \left. \frac{\partial \epsilon_{oL}}{\partial \omega} \right|_{\omega_0} + \frac{1}{2}(\omega - \omega_0)^2 \left. \frac{\partial^2 \epsilon_{oL}}{\partial \omega^2} \right|_{\omega_0} \\ \epsilon_e(\omega) &= \epsilon_{eL} + (\omega - \omega_0) \left. \frac{\partial \epsilon_{eL}}{\partial \omega} \right|_{\omega_0} + \frac{1}{2}(\omega - \omega_0)^2 \left. \frac{\partial^2 \epsilon_{eL}}{\partial \omega^2} \right|_{\omega_0}\end{aligned}$$

but now let them be coupled by the fourth-order nonlinear susceptibility tensor. This is assumed to be instantaneous and thus nondispersive.

$$\vec{P}_{NL} = \epsilon_0 \overset{(3)}{\equiv} \vec{E} \vec{E} \vec{E}$$

Which results in a coupled vector non-paraxial wave equation:

$$\begin{aligned}\nabla_{xyz}^2 \vec{E} - \nabla_{xyz} (\nabla_{xyz} \cdot \vec{E}) - \frac{1}{c^2} \left\{ \begin{bmatrix} \epsilon_{oL} & 0 & 0 \\ 0 & \epsilon_{oL} & 0 \\ 0 & 0 & \epsilon_{eL} \end{bmatrix} \right. \\ \left. + (\omega - \omega_0) \begin{bmatrix} \frac{\partial \epsilon_{oL}}{\partial \omega} & 0 & 0 \\ 0 & \frac{\partial \epsilon_{oL}}{\partial \omega} & 0 \\ 0 & 0 & \frac{\partial \epsilon_{eL}}{\partial \omega} \end{bmatrix} + \frac{1}{2}(\omega - \omega_0)^2 \begin{bmatrix} \frac{\partial^2 \epsilon_{oL}}{\partial \omega^2} & 0 & 0 \\ 0 & \frac{\partial^2 \epsilon_{oL}}{\partial \omega^2} & 0 \\ 0 & 0 & \frac{\partial^2 \epsilon_{eL}}{\partial \omega^2} \end{bmatrix} \right\} \frac{\partial^2 \vec{E}}{\partial t^2} \\ = \frac{1}{c^2} \frac{\partial^2}{\partial t^2} \left(\overset{(3)}{\equiv} \vec{E} \vec{E} \vec{E} \right)\end{aligned}$$

Small perturbation and phase matching

Assume perturbations are small, which reduces previous equation to two coupled scalar wave equations

$$\begin{aligned}\nabla_{xyz}^2 E_{(ord)} &= \frac{1}{c^2} \left[n_o^2 + (\omega - \omega_0) \frac{\partial n_o^2}{\partial \omega} + \frac{1}{2} (\omega - \omega_0)^2 \frac{\partial^2 n_o^2}{\partial \omega^2} \right] \frac{\partial^2 E_{(ord)}}{\partial t^2} \\ &= \frac{1}{c^2} \frac{\partial^2}{\partial t^2} \left(\Delta \chi_{(ord)jkl}^{(3)} E_j E_k E_l \right) \\ \nabla_{xyz}^2 E_{(ext)} &= \frac{1}{c^2} \left[n_e(\theta)^2 + (\omega - \omega_0) \frac{\partial n_e(\theta)^2}{\partial \omega} + \frac{1}{2} (\omega - \omega_0)^2 \frac{\partial^2 n_e(\theta)^2}{\partial \omega^2} \right] \frac{\partial^2 E_{(ext)}}{\partial t^2} \\ &= \frac{1}{c^2} \frac{\partial^2}{\partial t^2} \left(\Delta \chi_{(ext)jkl}^{(3)} E_j E_k E_l \right)\end{aligned}$$

In an anisotropic material, only a few terms of the nonlinear perturbation are phase matched

$$P_x^{(3)}(\vec{r}, t) = 3 \epsilon_0 \chi_{1121}^{(3)} \mathcal{E}_1 \mathcal{E}_2 \mathcal{E}_1^* e^{-j(\vec{k}_{(ord)} + \vec{k}_{(ext)} - \vec{k}_{(ord)}) \cdot \vec{r}} e^{j\omega t} + 7 \text{ other terms}$$

allowing us to collapse the 4th order tensor expression to self and cross-phase modulation indices:

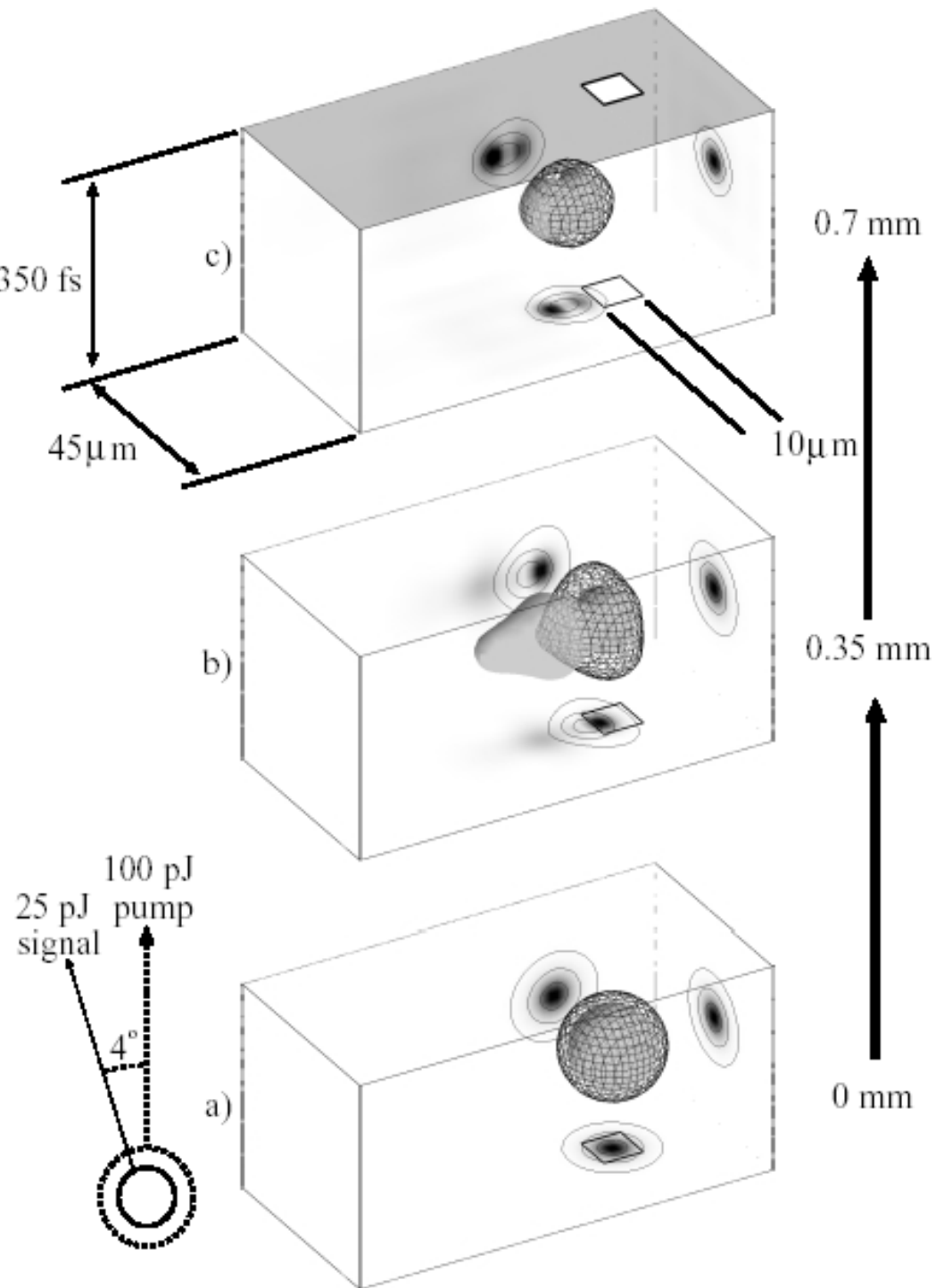
$$n_{(ord)} = n_o + n_{o2}^{\text{self}} |\mathcal{E}_1|^2 + n_{o2}^{\text{cross}} |\mathcal{E}_2|^2$$

$$n_{(ext)} = n_e(\theta) + n_{e2}^{\text{self}} |\mathcal{E}_2|^2 + n_{e2}^{\text{cross}} |\mathcal{E}_1|^2$$

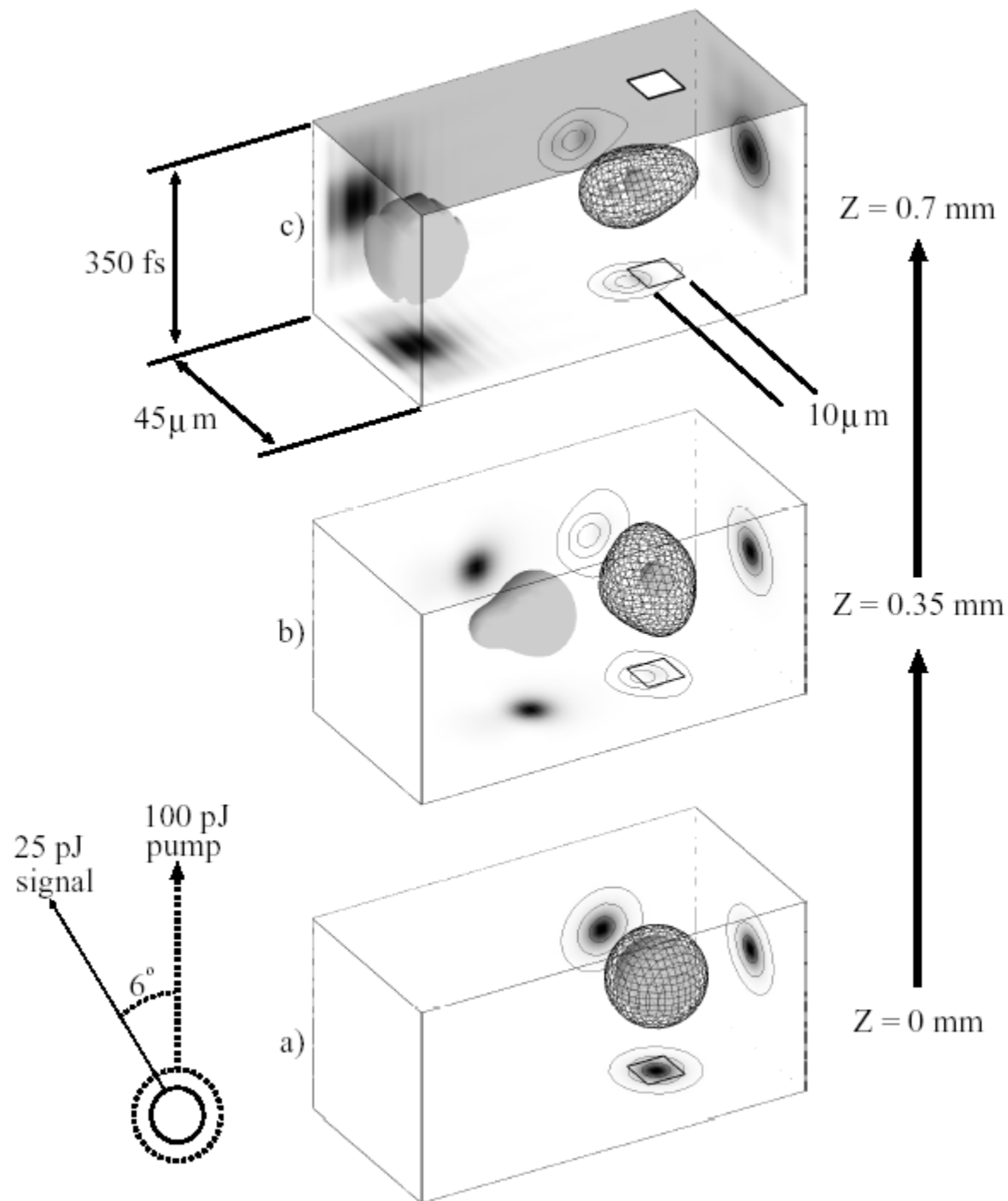
resulting in two coupled NLS equations

$$\begin{aligned}-j \frac{\partial u_{ord}}{\partial \zeta} + \frac{1}{2} \nabla_{\xi\eta\tau}^2 u_{ord} + \left(|u_{ord}|^2 + \frac{n_{2,ord}^{\text{cross}}}{n_{2,ord}^{\text{self}}} |u_{ext}|^2 \right) u_{ord} &= 0 \\ -j \frac{\partial u_{ext}}{\partial \zeta} + \frac{1}{2} \nabla_{\xi\eta\tau}^2 u_{ext} + \left(|u_{ext}|^2 + \frac{n_{2,ext}^{\text{cross}}}{n_{2,ext}^{\text{self}}} |u_{ord}|^2 \right) u_{ext} &= 0\end{aligned}$$

Interaction of two light-bullets Small angle



Interaction of two light-bullets Large angle



Spatio-temporal BPM in anisotropic, nonlinear media

1. Transform into group-velocity and anisotropic walk-off coordinate system
 - a) Removes first-order terms in k_z
2. Propagate two polarizations in independent spaces
 - a) Polarization basis should be eigenpolarizations of unperturbed medium
3. Couple polarizations by nonlinearity calculated in real-space for each grid

Energy conservation

I prefer to add an explicit absorber at each plane rather than a complex δn , but they are equivalent.

$$E(x,y,z + \Delta z) = \mathcal{F}_{xy}^{-1} \left\{ \mathcal{F}_{xy}[E(x,y,z)] e^{-jk_z(\omega, k_x, k_y)\Delta z} \right\} e^{-jk_0 \delta n(x,y,z + \Delta z/2)\Delta z} T(x,y,z + \Delta z/2)$$

Diffraction
Refraction
Transmission

Using Parseval's theorem and the fact that δn and k_z are real. Note k_z real only for propagating fields (not evanescent) – power is lost for evanescent modes.

$$\begin{aligned} \iint_{-\infty}^{\infty} |E(x,y,z)|^2 dx dy &= \iint_{-\infty}^{\infty} \left| \mathcal{F}_{xy}[E(x,y,z)] \right|^2 dk_x dk_y && \text{Parseval} \\ &= \iint_{-\infty}^{\infty} \left| \mathcal{F}_{xy}[E(x,y,z)] e^{-jk_z(\omega, k_x, k_y)\Delta z} \right|^2 dk_x dk_y && k_z \text{ real} \\ &= \iint_{-\infty}^{\infty} \left| \mathcal{F}_{xy}^{-1} \left\{ \mathcal{F}_{xy}[E(x,y,z)] e^{-jk_z(\omega, k_x, k_y)\Delta z} \right\} \right|^2 dx dy && \text{Parseval} \\ &= \iint_{-\infty}^{\infty} \left| \mathcal{F}_{xy}^{-1} \left\{ \mathcal{F}_{xy}[E(x,y,z)] e^{-jk_z(\omega, k_x, k_y)\Delta z} \right\} e^{-jk_0 \delta n \Delta z} \right|^2 dx dy && \text{dn real} \\ &= \iint_{-\infty}^{\infty} \frac{|E(x,y,z + \Delta z)|^2}{|T(x,y,z + \Delta z/2)|^2} dx dy && \text{FFT-BPM algorithm} \\ &&& \text{(from above)} \end{aligned}$$

Let the field just after the transmission mask be E' : $E'(x,y,z) = E(x,y,z) T(x,y)$

$$\iint_{-\infty}^{\infty} |E'(x,y,z + \Delta z)|^2 dx dy = \iint_{-\infty}^{\infty} |T(x,y,z)|^2 |E(x,y,z)|^2 dx dy$$

- Fourier beam propagation
 - Enhancements to method
 - TM propagation

1+1 dimensional TM propagation

Exact equations for TE (top) and TM (bottom) fields:

$$\nabla^2 E_y + k_0^2 n^2 E_y = 0$$

$$\nabla^2 H_y + k_0^2 n^2 H_y - \frac{1}{n^2} \frac{\partial n^2}{\partial z} \frac{\partial H_y}{\partial z} - \frac{1}{n^2} \frac{\partial n^2}{\partial x} \frac{\partial H_y}{\partial x} = 0$$

Let us make a substitution in the TM wave equation

$$H_y(x, z) = n(x, z) F(x, z)$$

We now find that the “field” F satisfies the following wave equation:

$$\nabla^2 F + k_0^2 n_{equiv}^2 F = 0$$

where

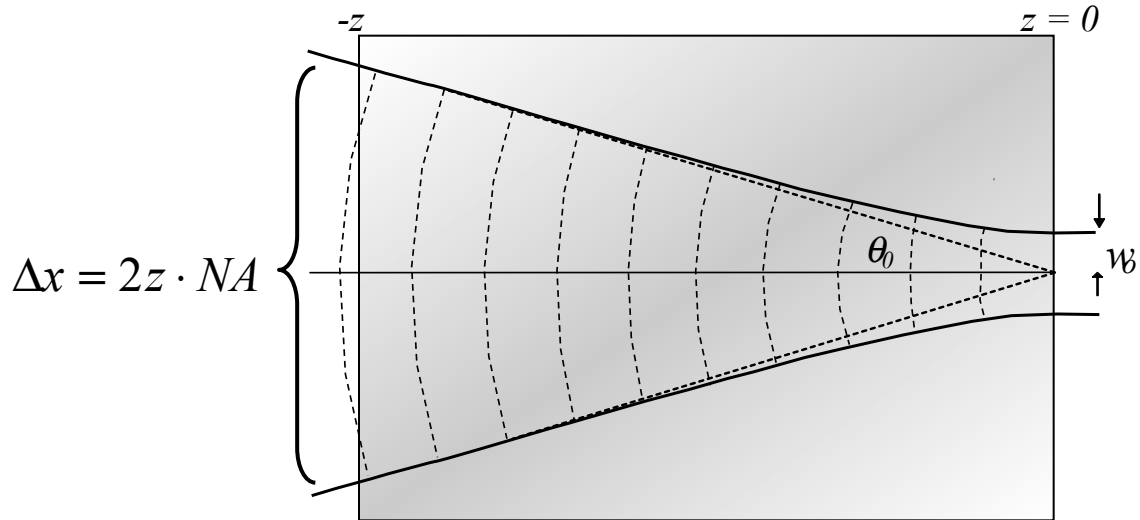
$$n_{equiv}^2(x, z) = n^2(x, z) - \frac{n^2(x, z)}{k_0^2} \nabla^2 \left[\frac{1}{n(x, z)} \right]$$

Which can now be propagated in our regular scalar/TE BPM. Note that the equivalent index is singular at material discontinuities. I usually handle this by smoothing my waveguides slightly (typically with a second-order interpolation to the step).

BPM of di/converging waves

Required spatial sampling

Consider the problem of modeling a converging wave:



To avoid aliasing of phase fronts at the edge of the converging beam, let the phase difference between adjacent cells at edge of beam be $< \pi$

$$\begin{aligned}
 \frac{2\pi}{\lambda_0} [r_{N/2+1} - r_{N/2}] &= \frac{2\pi}{\lambda_0} \left\{ \sqrt{[\delta x(N/2 + 1)]^2 + z^2} - \sqrt{[\delta x(N/2)]^2 + z^2} \right\} \\
 &\approx \frac{2\pi}{\lambda_0} \frac{[\delta x(N/2 + 1)]^2 - [\delta x(N/2)]^2}{2z} && \text{Binomial} \\
 &\approx \frac{\pi}{\lambda_0 z} \delta x^2 N && \text{Keep term of order } N \\
 &= \frac{2\pi}{\lambda_0} \delta x N A && (\delta x N)/(2z) = NA \\
 &< \pi && \text{Nyquist sampling}
 \end{aligned}$$

$$\delta x < \frac{\lambda_0}{2NA} = \frac{\pi}{2} w_0$$

Sampling must be $\sim w_0$ IN ALL SPACE

BPM of di/converging waves

Number of samples required

$$\begin{aligned}
 N_x &= \frac{\Delta x}{\delta x} && \text{\# of cells in one transverse direction.} \\
 &> \frac{(2z \cdot NA)}{\left(\frac{\lambda_0}{2NA}\right)} && \text{From previous page.} \\
 &= \frac{4NA^2}{\lambda_0} z \\
 &= \frac{4}{\pi} \left(\frac{z}{z_0} \right) && \text{Using expression for } z_0 \\
 &\approx \frac{z}{z_0} && \text{Number of cells along one side is equal to} \\
 &&& \text{distance from focus in units of Rayleigh range:}
 \end{aligned}$$

$$N_x N_y > \left(\frac{z}{z_0} \right)^2$$

Fine sampling and large beam size result in excessive memory requirements.

Example: 0.6 NA beam 4 mm from focus

$$\begin{aligned}
 N_x N_y &> (4000/0.47)^2 = 8500^2 = 72M \text{ cells} \\
 &= \frac{1}{2} \text{ GB single precision complex for single } z \text{ plane} \\
 &= 1 \text{ GB min unless using in-place FFT}
 \end{aligned}$$

Sziklas and Siegman algorithm

Mapping of converging to regular propagation

The Gaussian beam

$$E(\vec{r}) = A_0 \frac{w_0}{w(z)} e^{-\frac{x^2+y^2}{w^2(z)} - jkz - jk \frac{x^2+y^2}{2R(z)} + j\zeta(z)} \quad R(z) \equiv z \left[1 + \left(\frac{z_0}{z} \right)^2 \right]$$

is a solution to the homogeneous paraxial wave equation

$$-2jk \frac{\partial}{\partial z} E + \nabla_{xy}^2 E = 0$$

This motivates a coordinate transform in which the parabolic phase curvature is removed from the field:

$$E'(x', y', z') = z e^{+j \frac{k}{2z} (x'^2 + y'^2)} E(x, y, z)$$

The new field E' obeys the paraxial wave equation

$$-2jk \frac{\partial}{\partial z'} E' + \nabla_{x'y'}^2 E' = 0$$

if

$$x' \equiv \alpha \frac{x}{z}, \quad y' \equiv \alpha \frac{y}{z}, \quad z' \equiv \alpha^2 \frac{z - z_{Origin}}{z z_{Origin}}$$

z coordinate here is measured from focus, so this implies that an invariant coordinate grid x' would converge approaching focus and diverge leaving focus like

$$x = \frac{z}{\alpha} x'$$

Sziklas and Siegman algorithm

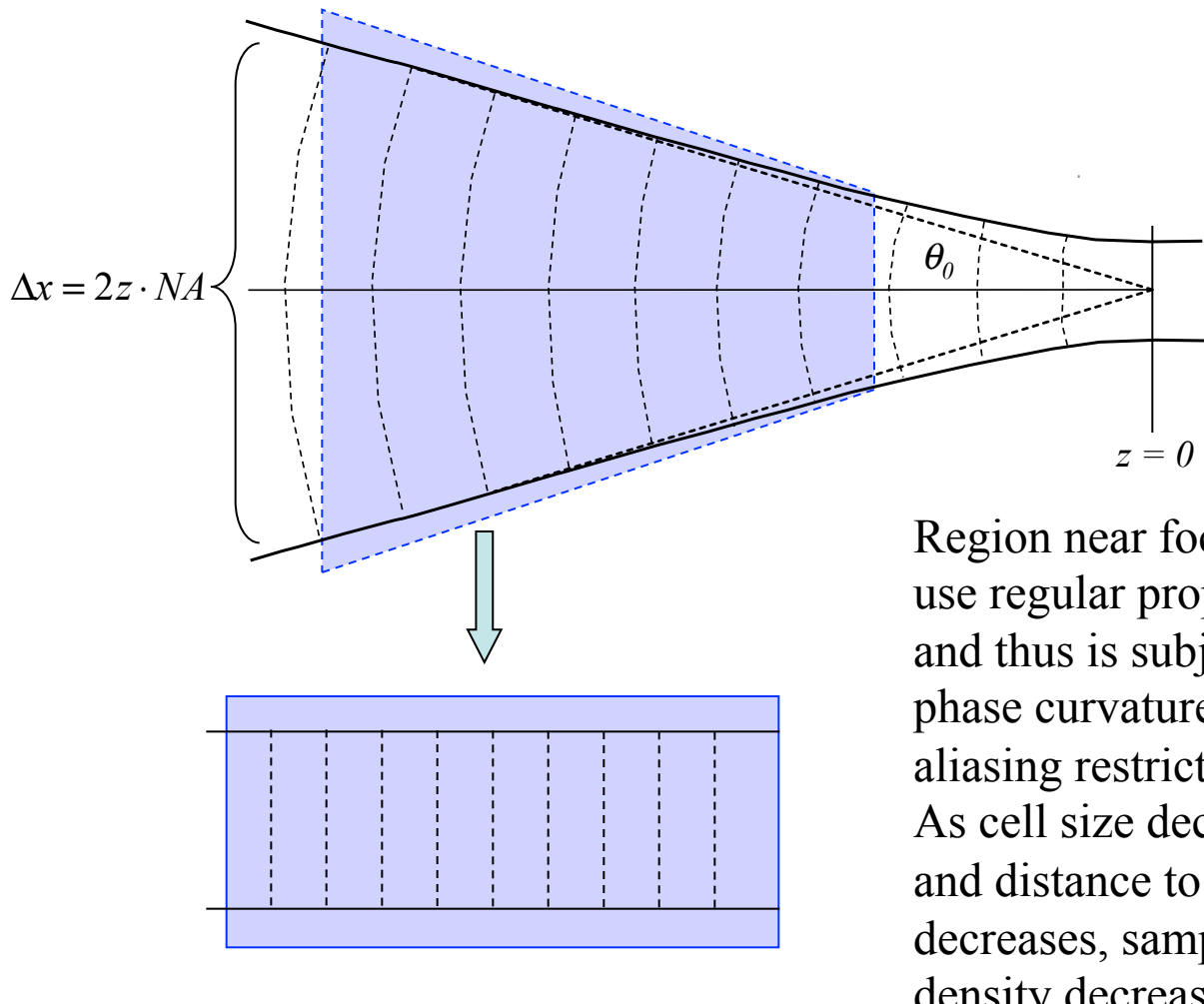
Mapping of converging to regular propagation

Divide field by Gaussian phase matched in curvature to field

Propagate in uniform (not converging space).

Cell size dynamically changes proportional to distance from focus:

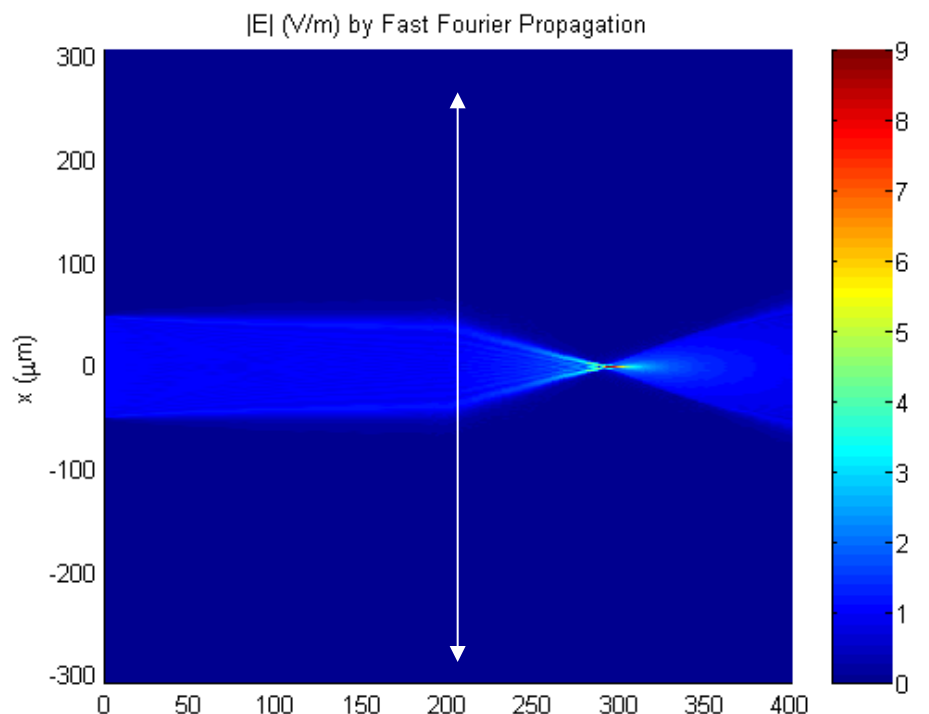
$$\delta x(z) = \delta x_{inc} \left(\frac{z}{z_{inc}} \right)$$



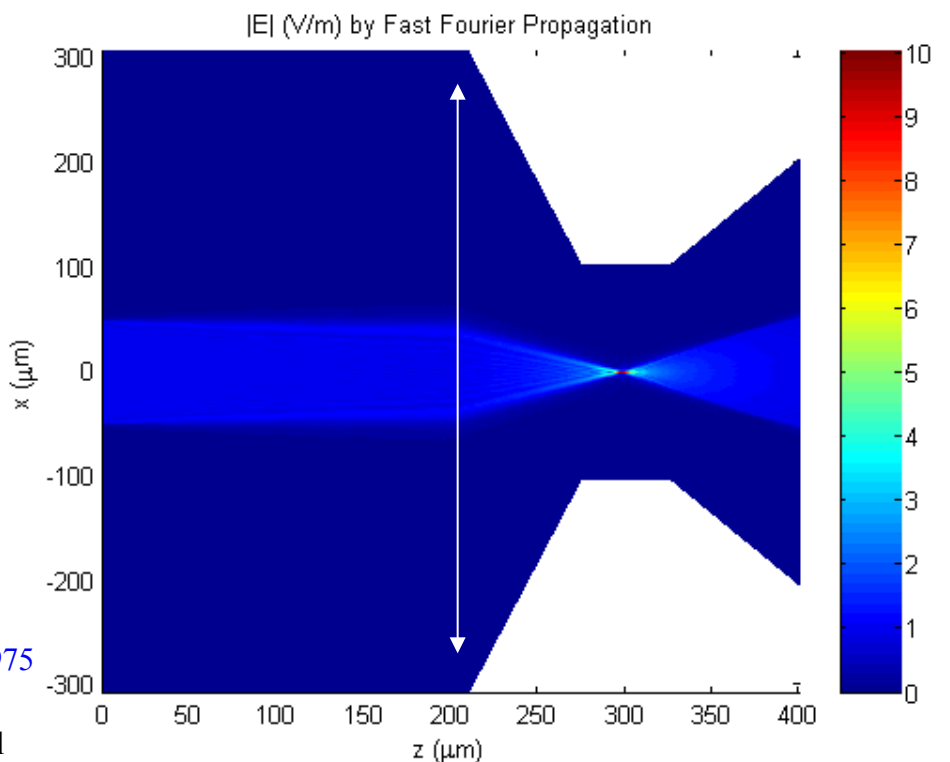
Sziklas and Siegman algorithm An adaptive grid for spherical waves

Non-paraxial imaging of a rectangular aperture in 1+1 dimensions

Regular FFT
propagation



Sziklas FFT
propagation

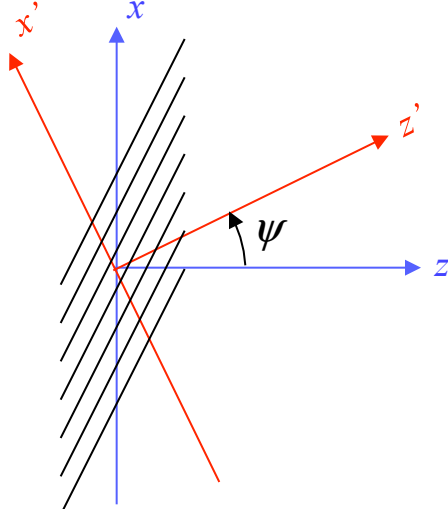


E. A. Sziklas, A. E. Siegman
Applied Optics 14, pp. 1874-1889, 1975

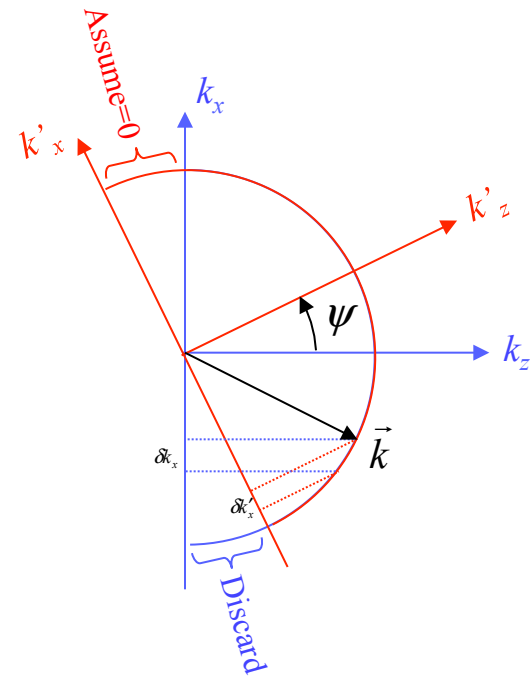
- Fourier beam propagation
 - Enhancements to method
 - Imaginary distance method

Tilted planes

Fourier-space rotation



Real space



Fourier space

$$\begin{bmatrix} x' \\ y' \\ z' \end{bmatrix} = \bar{\bar{R}} \begin{bmatrix} x \\ y \\ z \end{bmatrix} = \begin{bmatrix} \cos\psi & 0 & -\sin\psi \\ 0 & 1 & 0 \\ \sin\psi & 0 & \cos\psi \end{bmatrix} \begin{bmatrix} x \\ y \\ z \end{bmatrix}$$

Coordinate transformation for a point
P to a point P'

$$\vec{k}' = \bar{\bar{R}} \vec{k}$$

Then in Fourier space

$$\begin{aligned} k'_x &= k_x \cos\psi - \sqrt{k^2 - k_x^2} \sin\psi \\ &\approx -k \sin\psi + k_x \cos\psi + \left(\frac{k_x^2}{2k} + \frac{k_x^4}{8k^3} + \frac{k_x^6}{16k^5} + \dots \right) \sin\psi \end{aligned}$$

Sampling in new space is not regular
even to first order in ψ

Thus must interpolate back to regular grid in k'_x which is not numerically accurate

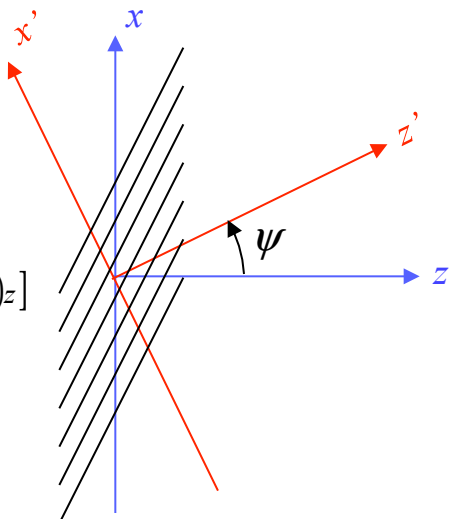
- Fourier beam propagation
 - Enhancements to method
 - Tilted planes

Tilted planes

Real-space propagation version

Write the free-space propagation algorithm:

$$\begin{aligned}
 E(x,y,z) &= \mathcal{F}_{xy}^{-1} \left\{ \mathcal{F}_{xy}[E(x,y,0)] e^{-jk_z(\omega, k_x, k_y)z} \right\} \\
 &= \mathcal{F}_{xy}^{-1} \left\{ E(k_x, k_y, z=0) e^{-jk_z(\omega, k_x, k_y)z} \right\} \\
 &= \sum_{k_x, k_y} E(k_x, k_y, z=0) e^{-j[k_x x + k_y y + k_z(\omega, k_x, k_y)z]} \\
 &= \sum_{k_x, k_y} E(k_x, k_y, z=0) e^{-j\vec{k} \cdot \vec{r}}
 \end{aligned}$$



Define the new tilted plane as a set of vectors that regularly sample the space

$$\vec{r}_{m,n} = m\delta x' \hat{x}' + n\delta y' \hat{y}'$$

And use the propagation formula to find E on this tilted, regularly sampled grid

$$E(x' = m\delta x', y' = n\delta y') = \sum_{k_x, k_y} E(k_x, k_y, z=0) e^{-j\vec{k} \cdot \vec{r}_{m,n}}$$

This is an irregular, discrete inverse FT. The sum is over the regularly sampled spatial frequencies k_x and k_y . As shown on the previous page, those spatial frequencies in (x, y, z) that correspond to evanescent waves or backwards traveling waves in (x', y', z') should be discarded.

Now use a regular FFT to find the spectrum for propagation in the tilted coordinates

$$E(k'_x, k'_y, z=0) = \mathcal{F}_{x'y'}[E(x', y', 0)]$$

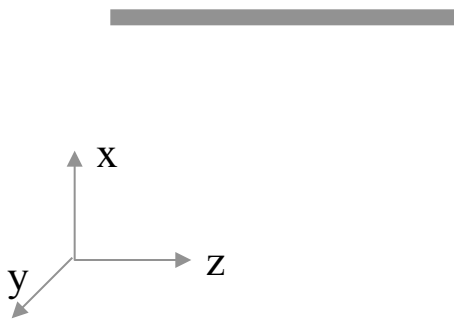
Note that for E in the x, z plane there will also be a polarization projection.

- Fourier beam propagation
 - Enhancements to method
 - Curved propagation

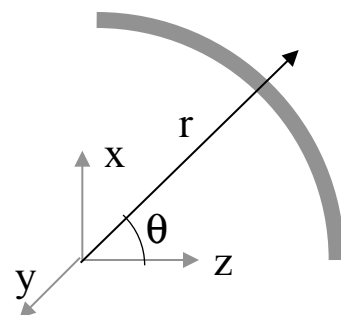
Propagating in curved spaces

Heuristic derivation

Straight waveguide



Bent waveguide, radius R



The waves propagating in the curved space accumulate extra phase proportional to distance from the center of the waveguide.

$$E(x, y, z) = E(x, y, 0)e^{-jk_0 \delta n(x)z}$$

Usual propagator

$$E(x, y, r \theta) = E(x, y, 0)e^{-jk_0 \delta n(x)r \theta}$$

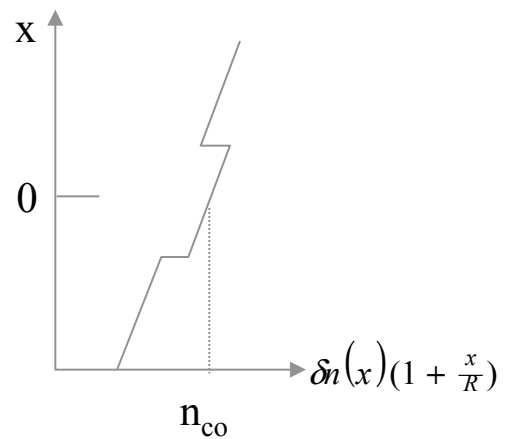
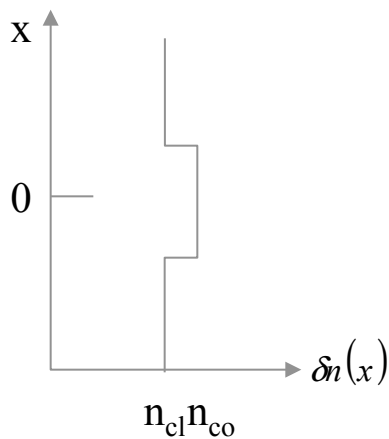
Equivalent in curved space

$$= E(x, y, 0)e^{-jk_0 \delta n(x)(R+x)(z/R)}$$

Map to prev. coordinates

$$= E(x, y, 0)e^{-jk_0 [\delta n(x)(1+\frac{x}{R})]z}$$

Equivalent index



Thus we can simulate (and understand) curved waveguides via a scaled dn.

- Fourier beam propagation
 - Enhancements to method
 - Curved propagation

Propagating in curved spaces Conformal transform

Consider a field in a 2D (x, z) plane described by

$$\left[\nabla_{xz}^2 + k_0^2 n^2(x, z) \right] E(x, y) = 0$$

This formally applies only TE propagation of a field E_z given a physical structure that is invariant in y . With minor modifications, it can describe TM propagation or waveguides with confinement in the y direction via the effective index approximation.

Apply a conformal transformation to a new set of coordinates u (radial) and v (azimuthal). The proper transform is:

$$W \equiv u + jv = R_2 \ln \frac{Z}{R_2} = R_2 \ln \frac{x + jz}{R_2}$$

Which gives the new wave equation:

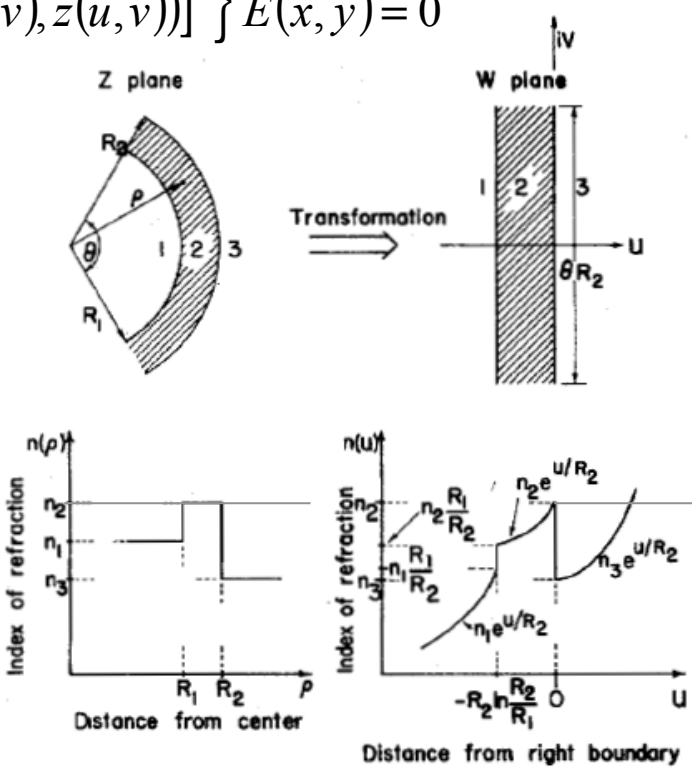
$$\left\{ \nabla_{uv}^2 + k_0^2 [e^{u/R_2} n(x(u, v), z(u, v))]^2 \right\} E(x, y) = 0$$

Application:

$$\begin{aligned} n(u) &= e^{u/R_2} n(\rho) \\ &\approx \left[1 + \frac{u}{R} + O(u^2) \right] n(\rho) \end{aligned}$$

which is the previous expression

$$\begin{aligned} u &= R_2 \ln \frac{\rho}{R_2} \\ v &= \theta R_2 \end{aligned}$$

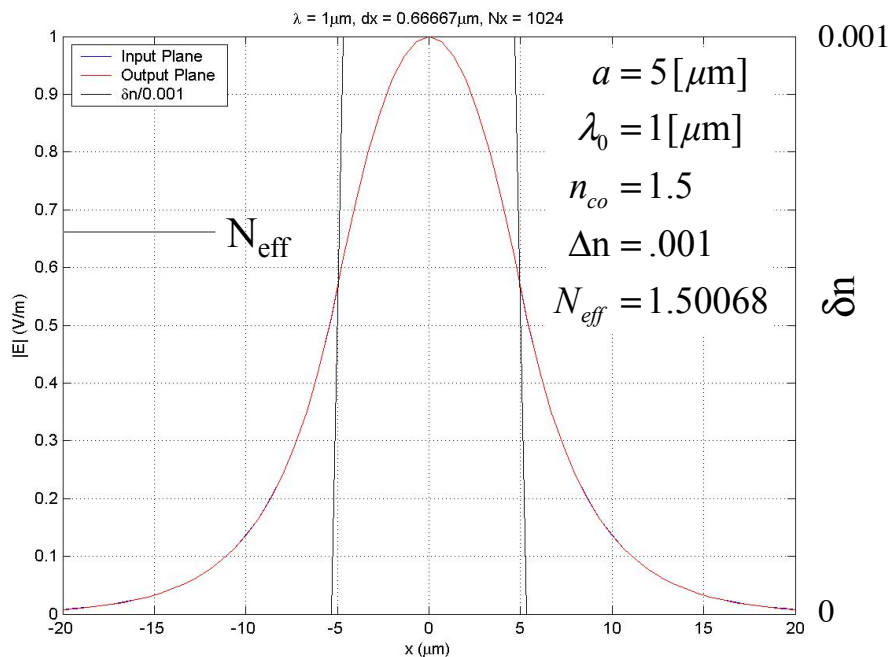


- Fourier beam propagation
 - Enhancements to method
 - Curved propagation

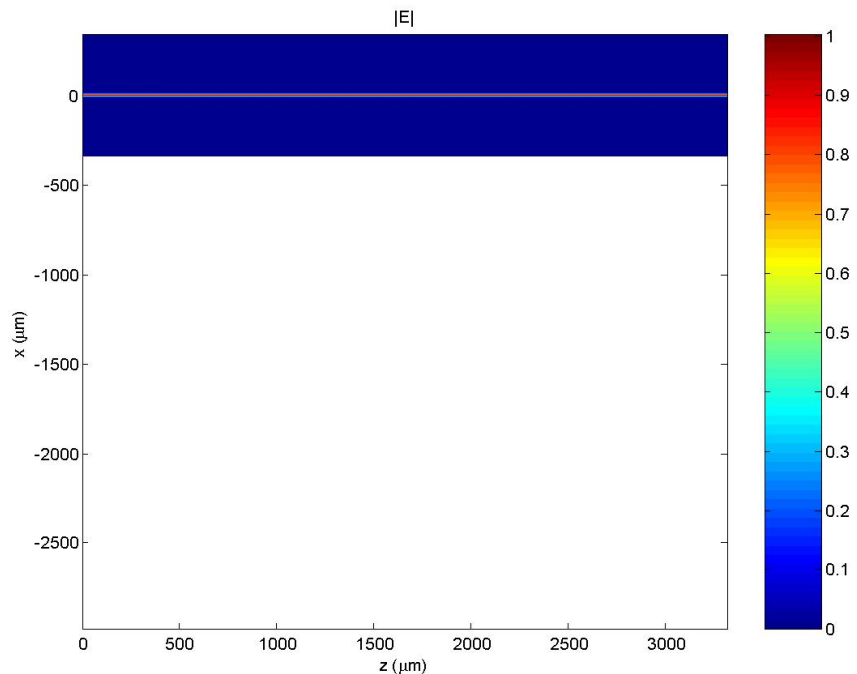
BPM in straight guide

Launch mode from slab waveguide solver.

Mode travels > 3mm without significant change.



$|E|$ vs. x,z

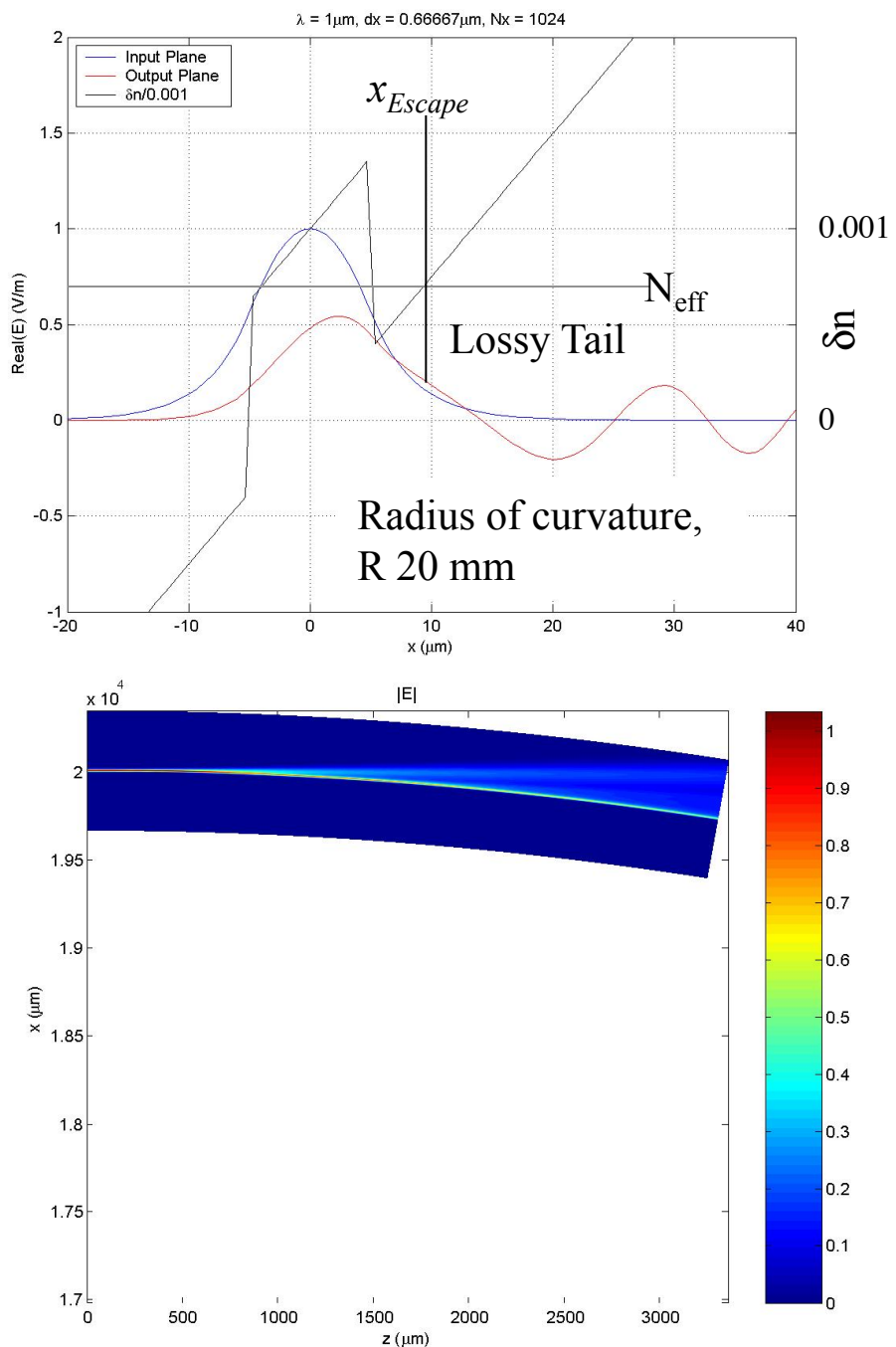


- Fourier beam propagation
 - Enhancements to method
 - Curved propagation

BPM in curved guide

Launch mode from slab waveguide solver.

Mode at exit is leaky, lower total power and shifted towards larger radius



$|E|$ vs. x, z . The plotting coordinate system has been warped to match the curvature of the space. The original propagation, however, is simply rectangular BPM with the index above.